

## **Tetraspanin CD63 acts as a pro-metastatic factor *via* $\beta$ -catenin stabilization**

Bastian Seubert<sup>1\*</sup>, Haissi Cui<sup>1\*</sup>, Nicole Simonavicius<sup>2</sup>, Katja Honert<sup>1</sup>, Sandra Schäfer<sup>1,3,4</sup>, Ute Reuning<sup>5</sup>, Mathias Heikenwalder<sup>2</sup>, Bernard Mari<sup>3,4</sup>, Achim Krüger<sup>1,6</sup>

<sup>1</sup>Institute for Experimental Oncology and Therapy Research and Institute of Molecular Immunology, Klinikum rechts der Isar der Technische Universität München, 81675 München, Germany

<sup>2</sup>Institute of Virology Technische Universität München/Helmholtz Zentrum München, 81675 München, Germany

<sup>3</sup>University of Nice Sophia-Antipolis, Nice, France.

<sup>4</sup>Institut de Pharmacologie Moléculaire et Cellulaire, Centre National de la Recherche Scientifique, 06560 Sophia Antipolis, France

<sup>5</sup>Clinical Research Unit, Department for Obstetrics and Gynecology, Technische Universität München, 81675 München, Germany

<sup>6</sup>Correspondence: [achim.krueger@lrz.tu-muenchen.de](mailto:achim.krueger@lrz.tu-muenchen.de)

\* These authors contributed equally.

### **Novelty and impact:**

We demonstrate that tetraspanin CD63 expression in tumor cells is necessary to maintain their capability to form metastatic colonies. CD63 is crucial for prevalence of the aggressive mesenchymal phenotype and regulates EMT via GSK3 $\beta$ -dependent  $\beta$ -catenin stabilization. Indeed, CD63 knock down mimics inhibition of  $\beta$ -catenin and PI3K/AKT or GSK3 $\beta$  inhibitors can rescue lack of CD63. This pro-metastatic role of CD63 renders this molecule as a possible target for interference with metastasis.

Conflict of interest: The authors have no conflict of interest.

### Abstract

The tetraspanin CD63 is implicated in pro-metastatic signaling pathways but, so far, it is unclear, how CD63 levels affect the tumor cell phenotype. Here, we investigated the effect of CD63 modulation in different metastatic tumor cell lines. *In vitro*, knock down of CD63 induced a more epithelial-like phenotype concomitant with increased E-cadherin expression, downregulation of its repressors Slug and Zeb1, and decreased N-cadherin. In addition,  $\beta$ -catenin protein was markedly reduced, negatively affecting expression of the target genes MMP-2 and PAI-1.  $\beta$ -catenin inhibitors mimicked the epithelial phenotype induced by CD63 knock down. Inhibition of  $\beta$ -catenin upstream regulators PI3K/AKT or GSK3 $\beta$  could rescue the mesenchymal phenotype underlining the importance of the  $\beta$ -catenin pathway in CD63-regulated cell plasticity. CD63 knock down-induced phenotypical changes correlated with a decrease of experimental metastasis while CD63 overexpression enhanced the tumor cell-intrinsic metastatic potential. Taken together, our data show that CD63 is a crucial player in the regulation of the tumor cell-intrinsic metastatic potential by affecting cell plasticity.

## Introduction

Metastasis is the major cause of death in cancer patients suffering from solid tumors<sup>1</sup>.

Epithelial-mesenchymal transition (EMT) is a prerequisite for successful dissemination and colonization of secondary organs by tumor cells<sup>2</sup>. EMT has been shown to result in increased cancer cell motility by reorganization of actin filaments, downregulation of E-Cadherin, and increased expression of N-Cadherin<sup>2-4</sup>. Molecular regulators of EMT are the transcription factors Snail, the bHLH and ZFH protein families (Zeb1 and Zeb2) which suppress the gene expression signature assigned to the epithelial phenotype<sup>3,5</sup>. MicroRNAs (miRNAs), including members of the miR-200 family, for example miR-141, have been shown in turn to suppress Zeb proteins, adding an additional level of regulation<sup>6</sup>. In addition,  $\beta$ -Catenin, which is regulated by Glycogen synthase kinase 3 beta (GSK3 $\beta$ ) phosphorylation<sup>7</sup>, is shown to play a decisive role in EMT-induction by its ability to both, sense E-Cadherin status and control gene expression of target genes like MMP-2 and PAI-1<sup>4</sup>. EMT is regulated by different cytokines and growth factors, including TGF- $\beta$ 1<sup>3</sup>. Mesenchymal-to-epithelial transition (MET) gained recognition as a crucial process for successful metastasis formation, as tumor cells switch back to a more epithelial phenotype at the site of metastatic outgrowth<sup>5</sup>. Therefore, cellular plasticity and regulation of these alternating phenotypes are of importance during metastatic cancer progression<sup>5</sup>.

Tetraspanins seem to play a role in cancer progression. Some family members are described to exert pro-metastatic properties, while others are reported to inhibit metastasis<sup>8</sup>. This protein family displays four membrane-spanning domains and their ability to form multiprotein complexes by interacting with other tetraspanins and also with a variety of other transmembrane and cytosolic proteins<sup>9-11</sup>. Tetraspanins are involved in many biological processes, including cell adhesion, migration, cell fusion, as well as signal transduction by interacting with partner molecules<sup>9,10</sup>. The family member CD63 is of special interest as it is found to be upregulated in patients suffering from breast cancer<sup>12</sup>, astrocytoma<sup>13</sup>, or

melanoma<sup>14,15</sup>. CD63 is ubiquitously expressed and is localized in membranes of endosomes and exosomes, as well as at the cell surface<sup>16</sup>. While CD63 has been originally described as a tumor suppressor<sup>17-22</sup>, its function is worthwhile to be reassessed as it was identified as a receptor of tissue inhibitor of metalloproteinases-1 (TIMP-1)<sup>23</sup>, which may execute metastasis-promoting functions<sup>24</sup>. On the basis of these novel observations and its involvement in pro-tumorigenic cell signaling, including activation of phosphoinositide 3-kinases (PI3K)<sup>25</sup>, extracellular signal-regulated kinases (ERK)<sup>23,26</sup>, and  $\beta$ -catenin<sup>27</sup>, it may be hypothesized that CD63 modulation may affect pro-metastatic tumor cell properties.

In the present study, we show that CD63 levels impact on the maintenance of an epithelial or mesenchymal phenotype in tumor cells, thus acting as a pro-metastatic factor decisively influencing the success of metastatic tumor cell colonization.

## Materials and Methods

### Stable transduction of tumor cell lines

Human ovarian carcinoma cell lines (SKOV3ipL<sup>28</sup>), human gastric carcinoma cells (GTL-16L), and B16F10L mouse melanoma cells (both obtained from ATCC-LGC Standards, Wesel, Germany) cells were generated by transduction with the bacterial *lacZ* gene and cultured according to the distributor's instruction or as described previously<sup>29</sup>. Transfection of 293T cells for production of lentiviral particles has been described in detail elsewhere<sup>28</sup>. Cells were infected with lentiviral particles with a multiplicity of infection of approximately 5 and in the presence of 8  $\mu$ g polybrene (Sigma Aldrich, Munich, Germany). Knock down of CD63 was performed using lentiviral vectors purchased from Sigma Aldrich, Munich, Germany (TRCN0000007849, TRCN0000007851, TRCN0000065683 (shCD63\_1), TRCN0000065687 (shCD63\_5). shRNA which does not target any known human or mouse gene (shNT, Sigma Aldrich, Munich, Germany) was used as a control. The following cell lines were generated for the present study, with a stable knock down of CD63 or the respective shNT control:

SKOV3ipL\_sh49, SKOV3ipL\_sh51, and SKOV3ipL\_shNT, B16F10L\_shNT, B16F10L\_sh1, B16F10L\_sh5. SKOV3ipL\_SFCD63 were generated as SKOV3ipL cells with a stable overexpression of CD63 and the control cell lines SKOV3ipL\_SF. CD63 overexpressing cells were generated using the third-generation self-inactivating lentiviral vector pRRL.PPT.SF.CD63 which contains a spleen focus-forming virus promoter<sup>30</sup>. Lentiviral particles based on the respective empty vector were used as controls.

### **Experimental metastasis assay**

$1 \times 10^6$  SKOV3ipL cells (knock down or overexpression of CD63 or the respective non-target or empty vector control) were inoculated into the tail vein of pathogen-free, female NMRI<sup>nu/nu</sup> mice (Charles River, Sulzfeld, Germany).  $2 \times 10^5$  B16F10L cells were analogously inoculated into pathogen-free, *syngeneic*, female C57Bl/6 mice (Charles River, Sulzfeld, Germany). Mice were sacrificed 24 h (SKOV3ipL, homing), 35 days (SKOV3ipL, outgrowth of metastases), and 14 days (B16F10L, outgrowth of metastases) after tumor cell inoculation, respectively. All organs were removed, liver and lungs were snap-frozen in liquid nitrogen, parts of all organs in the abdominal cavity and chest were stained in X-Gal solution<sup>28</sup>, and liver and lung pieces were prepared for immunohistochemical analysis.

### **Ethics statement**

All experiments were performed in compliance with the guidelines of the *Tierschutzgesetz des Freistaates Bayern* and were approved by the *Regierung von Oberbayern* (permission number: 55.2-1-54-2531-69-05; 55.2-1-54-2531-72-08; 55.2-1-54-2531-13-09; 55.2-1-54-2531-143-11, 55.2-1-54-2531-91-13) and all efforts were made to minimize suffering.

### **Cellular assays**

For analysis of proliferation,  $1 \times 10^3$  SKOV3ipL-derived cells/well or  $2.5 \times 10^3$  B16F10L-derived cells/well were seeded on 96-well cell culture plates in 100  $\mu$ l of media supplemented with 10% fetal calf serum (FCS). Proliferation was analyzed at 0, 24, 48, and 72 hours by incubation with AlamarBlue® (Life Technologies, Darmstadt, Germany) for 2 hours and

measured in a microtiter plate reader (PerkinElmer, Rodgau, Germany) according to the manufacturer's protocol.

For analysis of cell viability,  $1 \times 10^4$  SKOV3ipL-derived cells or  $2.5 \times 10^4$  B16F10L-derived cells/well were seeded on 96-well plates and incubated in medium supplemented with 0.5% FCS, the cells were incubated for 1 hour with AlamarBlue® (Life Technologies, Darmstadt, Germany) at the indicated time points and viability measured in a microtiter plate reader (PerkinElmer, Rodgau, Germany) according to the manufacturer's protocol.

For analysis of signaling pathways, the following small molecule inhibitors were used: Wortmannin (0.1  $\mu\text{M}$ ) and Ly294002 (1  $\mu\text{M}$ , both Sigma Aldrich, Munich, Germany, dissolved in dimethylsulfoxide (DMSO)) were administered to the media of the respective cell line for 24 hours. Quercetin (20  $\mu\text{M}$ , Santa Cruz Biotechnology, Heidelberg, Germany, dissolved in DMSO) was added to the media of the respective cell lines for 24 hours. Specific GSK3 inhibitors SB-216763 (25  $\mu\text{M}$ , Santa Cruz Biotechnology, Heidelberg, Germany, dissolved in DMSO) were applied on the respective cell line for 24 hours. The corresponding amount of DMSO was used as a control in all cases.

Migration assays were performed using Costar Transwell Permeable Supports with 8  $\mu\text{m}$  pore size (Corning Inc., Corning, NY, USA).  $2.5 \times 10^4$  SKOV3ipL-derived cells or  $1 \times 10^4$  B16F10L-derived cells were seeded in serum-free media. Media containing 10 % FCS (Biochrom, Berlin, Germany) was used as chemoattractant and added to the bottom chamber of 24-well cell culture plates. After an incubation time of 24 h (all human ovarian carcinoma cell lines) and 16 h (murine melanoma cell line) at 37 °C, non-migratory cells were removed using a cotton swab and migrated cells were fixed using Diff-Quik solution (Dade Behring, Marburg, Germany) and stained using 4',6-diamidino-2-phenylindole (DAPI, AppliChem, Darmstadt, Germany).

Invasion assays were performed using Costar Transwell Permeable Supports with 8  $\mu\text{m}$  pore size coated with 1 mg/mL BD Matrigel™ Basement Membrane Matrix (BD Biosciences,

Heidelberg, Germany).  $5 \times 10^4$  SKOV3ipL-derived cell lines or  $2 \times 10^4$  B16F10L-derived cell lines were seeded in serum-free media. Media containing 10 % FCS were used as chemoattractant added to the bottom chamber of 24 well plates. After an incubation time of 24 h at 37 °C, samples were processed as described above. At least 5 photos were taken of each insert at a 10-fold magnification and single cells were counted using Axiovision software (Carl Zeiss, Jena, Germany).

Clonogenic capacity of tumor cells was measured by seeding  $1 \times 10^3$  cells per well in 6-well plates. Cells were treated with 2  $\mu$ M cisplatin or the respective PBS control. After 7 to 10 days, colonies were fixed with 4 % PFA for 5 min at room temperature and stained with crystal violet (Roth, Karlsruhe, Germany) for 10 min. Cells were washed and colonies counted.

Scatter assays were performed by seeding 500 cells/well in a 6-well cell culture plate. Cells were incubated in the presence of 10% FCS for seven to ten days. Colony morphology was analyzed under the microscope. Colonies showing single cells with an elongated shape were counted as scattered colonies. At least 30 colonies were analyzed per well and number of scattered colonies per total number of colonies is shown.

#### **RNA isolation, reverse transcription, and qRT-PCR**

Total RNA from cells was isolated using TRIzol Reagent (Life Technologies, Darmstadt, Germany) according to the manufacturer's instructions. Reverse transcription for subsequent analysis of mRNA levels was performed using the High Capacity cDNA Reverse transcription Kit (Applied Biosystems, Frankfurt am Main, Germany). Primer design for qRT-PCR was done using ProbeFinder Software for Universal ProbeLibrary (all Roche Applied Science, Penzberg, Germany). miR-144 and U6 snRNP were amplified using Applied BiosystemsTaqMan MicroRNA Reverse Transcription Kit and measured with assays designed and inventoried by Applied Biosystems, Frankfurt am Main, Germany, according to the manufacturer's instruction.

### **Microarray analysis**

Parental SKOV3ipL cells, control shNT and the 2 shCD63 cell lines were seeded 24 hours prior to RNA isolation on a 10 cm dish. RNA was assessed for integrity by using an Agilent BioAnalyser 2100 (Agilent Technologies, Santa Clara, US) (RIN above 9). RNA samples were then labeled with Cy3 dye using the low RNA input QuickAmp kit (Agilent Technologies) as recommended by the supplier. 825 ng of labeled cRNA probe were hybridized on 8x60K high density SurePrint G3 v2 gene expression human microarrays. The experimental data are deposited in the NCBI Gene Expression Omnibus (GEO) (<http://www.ncbi.nlm.nih.gov/geo/>) under the series record number GSE61957. Normalization of microarray data was performed using the Limma package available from Bioconductor (<http://www.bioconductor.org>). Inter slide normalization was performed using the quantile methods. Means of ratios from all comparisons were calculated and B test analysis using paired analysis was performed. Differentially expressed genes were selected based on an adjusted p-value below 0.05 and an absolute value of  $\log_2$  (mean ratio) > 0.7. Data were analyzed for enrichment in biological themes (diseases and functions, canonical pathways, upstream analysis) using Ingenuity Pathway Analysis software (<http://www.ingenuity.com/>).

### **Western blot analysis**

Total protein was extracted upon cell lysis in cell signaling buffer (Cell Signaling, Frankfurt am Main, Germany). In order to minimize protein degradation and dephosphorylation, Protease Inhibitor (Roche, Penzberg, Germany) and phosphatase-inhibitors (Santa Cruz Biotechnology, Heidelberg, Germany) were added. Total protein concentration was assessed using a BCA assay (Thermo Scientific, Bonn, Germany). Western blotting was performed as described previously<sup>29</sup>. Primary antibodies against E-cadherin, N-cadherin, Slug, GSK3 $\alpha$  $\beta$ , PI3K110 $\alpha$ , and Snail, were purchased from Cell Signaling, Frankfurt am Main, Germany. For detection of GSK3 $\beta$ , AKT, and the respective phosphorylated versions the respective antibodies from Santa Cruz Biotechnology (Heidelberg, Germany) were used. Antibody

directed to  $\alpha$ -Tubulin antibody was obtained from Calbiochem Immunochemicals (Darmstadt, Germany). Co-immunoprecipitation of CD63 and integrins was performed using Anti-CD63 antibodies purchased from Santa Cruz Biotechnology. Mild detergent buffer consisted of standard Tris-buffered saline, 1 % Brij98 (Sigma Aldrich, Munich, Germany), 1 mM MgCl<sub>2</sub> and protease- and phosphataseinhibitors. Stringent conditions were achieved using the same basic buffer but with 1 % NP-40 instead of Brij98. Antibodies against Integrin  $\beta$ 1 and Integrin  $\beta$ 3 were distributed by Millipore, Darmstadt, Germany. Antibodies against  $\alpha$ v and Integrin  $\beta$ 5 were purchased from Biorbyt, Cambridge, UK. Isotype controls were purchased from Abcam (rabbit IgG, Cambridge, UK) and Thermo Scientific (mouse IgG, Bonn, Germany).

### **Immunostaining on cells**

For immunofluorescent analysis, cells were seeded on Superfrost® Plus glass slides (Thermo Scientific, Bonn, Germany) and stained with antibodies directed to PAI-1 (Santa Cruz Biotechnology, Heidelberg, Germany), Phospho-AKT (Santa Cruz Biotechnology, Heidelberg, Germany), Vimentin (Cell Signaling, Frankfurt am Main, Germany), Slug (Cell Signaling, Frankfurt am Main, Germany), or Zeb1 (Cell Signaling, Frankfurt am Main, Germany), respectively. Primary antibodies were visualized using AlexaFluor488-labeled rabbit secondary antibody (Invitrogen/Life Technologies, Darmstadt, Germany) or FITC-conjugated mouse secondary antibody (Invitrogen/Life Technologies, Darmstadt, Germany). Counterstaining was achieved with 1  $\mu$ g/ml 4',6-diamino-2-phenylindole (DAPI, Applichem, Darmstadt, Germany) and PhalloidinCruzFluor™ 488 Conjugate (Santa Cruz Biotechnology, Heidelberg, Germany) or RhodaminePhalloidin (Life Technologies, Darmstadt, Germany). Cells were mounted with Roti®-MountFluorCare (Roth, Karlsruhe, Germany). Fluorescent images were collected sequentially in one to three channels on a TCS-SP5 confocal microscope (Leica Microsystems, Wetzlar, Germany) at room temperature. For FACS analysis of  $\beta$ 1 and  $\beta$ 3, cells were stained using the same antibodies as used in Western blot analysis. Antibodies against  $\alpha$ v $\beta$ 3 and  $\alpha$ v $\beta$ 5 were distributed by Millipore, Darmstadt,

Germany. Secondary antibody used in FACS analysis was derived from Abcam, Cambridge, UK. Isotype controls were purchased from Abcam (rabbit IgG, Cambridge, UK) and Thermo Scientific (mouse IgG, Bonn, Germany). The following objectives were used: HCX PL APO CS 20.0x0.70 IMM UV, HCX PL APO CS 40.0x1.25 OIL UV. Images were exported from the Leica software (LAS AF Version: 2.6.0 build 7266).

### **Zymography**

Cathepsin zymography was performed as described previously<sup>31</sup>. MMP zymography has also been described elsewhere in detail<sup>32</sup>. In brief,  $2.5 \times 10^5$  cells were seeded on 6 cm plates and medium was conditioned for 24 hours and conditioned medium was loaded in gels containing gelatine.

### **Phosphokinase array**

Profiles of phosphokinases were analyzed using human phosphokinase arrays (R&D systems, Minneapolis, USA) according to the manufacturer's instructions. Protein lysates of SKOV3ipL cells were prepared using cell lysis buffer (Cell Signaling, Frankfurt am Main, Germany) according to the manufacturer's protocol. Protein lysates were incubated overnight with antibody array membranes displaying antibodies against 46 different phosphokinases. Horseradish peroxidase-conjugated secondary antibodies (GE Healthcare, Buckinghamshire, England) were used for detection with Lumi-light (Roche Diagnostics, Penzberg, Germany).

### **Statistical analysis**

Data were tested for normal distribution using the Shapiro-Wilk test. Normally distributed data were tested for statistical significance using an unpaired two-sample t-test. When normality distribution testing failed, One-way ANOVA was applied. GraphPad Prism 6 (GraphPad Software, Inc., La Jolla, USA) was used for all statistical tests.

## Results

### **Knock down of CD63 suppressed the metastatic potential of tumor cell lines of different origin.**

In order to investigate the role of CD63 for the metastatic potential of different tumor cell lines, we stably knocked down CD63 (Figure S1A-G) and performed experimental metastasis assays (Figure 1A-C). CD63 knock down markedly inhibited metastatic lung colonization of both, the human ovarian carcinoma cell line SKOV3ipL (Figure 1A) and the murine melanoma cell line B16F10L (Figure 1B). To further analyze at which stage of metastatic progression CD63 knock down was effective, we tested homing within 24 hours (Figure 1C) and used clonogenic assays to estimate colony formation ability (Figure 1D). Homing of tumor cells to the lung (Figure 1C) was only slightly affected while metastatic outgrowth was reduced (Figure 1A). *In vitro*, CD63 knock down reduced the colony forming ability of cells (Figure 1D, S2F) and decreased the resistance of SKOV3ipL cells against the chemotherapeutic agent cisplatin (Figure 1D) while cell proliferation was not affected (Figure S2A, B). In addition, expression of stem cell markers CD44 and CD117 (Figure S2C, D) was reduced, while CD24 was increased (Figure SE). Altogether, these findings suggest that CD63 knock down impacts on self-renewal factors and the capability of the tested tumor cell lines to form colonies *in vitro* and *in vivo*.

### **CD63 knock down decreased $\beta$ -catenin protein levels**

As  $\beta$ -catenin is a major regulator of self-renewal in cells and has been described to be regulated by CD63-dependent cell signaling<sup>27</sup>, we assessed  $\beta$ -catenin levels in CD63 knock down cells (Figure 2A-C).  $\beta$ -catenin protein levels were reduced upon CD63 knock down (Figure 2B, C, S3A, D), while mRNA levels did not change (Figure 2A). In addition, expression of the  $\beta$ -catenin downstream targets PAI-1<sup>33</sup> and MMP-2<sup>34</sup> was also reduced upon

CD63 knock down (Figure 2D, E, S3B, C). In order to better understand the consequences of CD63 knock down, we performed a whole transcriptome comparison of SKOV3ipL cells transduced with shRNA against CD63 compared to the shNT control. To avoid any potential off-target effects, we focused our attention on the pathways that were significantly deregulated in both SKOV3ipL\_shCD63\_49 and SKOV3ipL\_shCD63\_51 cells compared to SKOV3ipL\_shNT cells. Interestingly, biological function analysis using Ingenuity Pathway Analysis indicated an inhibition of biofunctions associated with cell movement, migration and invasion (Table S1). In agreement, several proteases were differentially regulated following CD63 knock down (Figure S4A-G, Table S2). As  $\beta$ -catenin protein levels are controlled by phosphorylation and subsequent ubiquitination by the upstream negative regulator kinase GSK3 $\beta$ <sup>7</sup>, we checked GSK3 $\beta$  and found decreased levels of inactive, phosphorylated GSK3 $\beta$  (Figure 2F, S3G) upon CD63 knock down. In addition, levels of phosphorylated  $\beta$ -catenin were increased (Figure S3E). As CD63 is described to regulate the activity of the PI3K pathway<sup>25</sup> and PI3K/AKT has been described to be connected with GSK3 $\beta$ -regulation<sup>35</sup>, we further assessed levels of class I PI3K P110 $\alpha$  and S473-phosphorylated AKT (Figure 2G). Both were decreased upon CD63 knock down. These data were consistent with the transcriptomic analysis showing a significant predicted inhibition of AKT1 according to Ingenuity Pathway Analysis (Table S3).

### **Knock down of CD63 led to mesenchymal-to-epithelial transition**

As  $\beta$ -catenin is a known inducer of EMT, we next analyzed morphological changes in SKOV3ipL and B16F10L cells upon CD63 knock down. Indeed, the shape of cells in colonies changed from elongated cells to an increased formation of cobblestone-like epithelial cell colonies upon CD63 knock down (Figure 3A, B, S5A, B). This indicated that CD63 may be involved in the maintenance of the mesenchymal-like phenotype. In order to test this on a molecular level, we next measured expression of the epithelial cell marker E-cadherin and

found that CD63 knock down led to an increase of E-cadherin on both, the mRNA (Figure 3C, D) and the protein level (Figure 3C). Concomitantly, the mesenchymal markers N-cadherin (Figure 3E, F), vimentin (Figure S5D), and fibronectin (S5E, F) were reduced. Microarray analysis indicated that expression of other tetraspanins was also differentially regulated (Figure S6A-D, Table S4), while integrins  $\beta 1$  and  $\beta 3$  (Figure S6E, F, Table S5), and the integrin heterodimers  $\alpha v\beta 3$  and  $\alpha v\beta 5$  (Figure S6 G, H) remained unchanged. As SKOV3ipL cells displayed the most obvious changes in cell shape and cytoskeleton rearrangements upon CD63 knock down (Figure S5C-D), we focused our analyses on this cell line. In order to identify upstream regulators of this cadherin switch, we assessed levels of known EMT-regulators and found the expression of the E-cadherin suppressors Slug and Zeb1 decreased upon CD63 knock down (Figure 3G, H, S5G-I). In addition, one miRNA of the miR-200 family, namely miR-141, was increased when CD63 was reduced (Figure 3I), while microRNA let7f 5p was not changed (Figure S3F). As a mesenchymal phenotype is also a prerequisite for cell motility<sup>2</sup>, we assessed cellular migratory activity using transwell assays and invasion through matrigel. Knock down of CD63 also reduced migration and invasion (Figure 3J, Table S6, S1).

### **CD63 regulated EMT via GSK3 $\beta$ -dependent $\beta$ -catenin stabilization**

TGF- $\beta 1$ , is a well-described inducer of EMT<sup>36</sup> which can influence tumor cell signaling by induction of  $\beta$ -catenin<sup>36</sup>. Interestingly, the epithelial phenotype induced by CD63 knock down was strong enough to override effects induced by TGF- $\beta 1$  incubation: both scattering of tumor cells and expression of  $\beta$ -catenin targets in response to TGF- $\beta 1$  were not increased in CD63 knock down cells (Figure 4A-C). In order to elucidate a functional connection between reduced  $\beta$ -catenin protein levels and the cadherin switch in CD63 knock down cells, we applied inhibitors against  $\beta$ -catenin and GSK3 $\beta$ . SKOV3ipL cells treated with the  $\beta$ -catenin inhibitor quercetin responded by adopting an epithelial cell-like morphology, the percentage

of scattered colonies was decreased (Figure 4D), and E-cadherin expression was induced (Figure 4E). CD63 knock down cells did not respond to quercetin treatment (Figure 4D, E). Inhibition of GSK3 $\beta$  activity by employing specific inhibitors (SB216763) led to rescue of the CD63 knock down phenotype in SKOV3ipL cells with respect to mesenchymal cell-like morphology, scattering potential (Figure 4F), and E-cadherin mRNA expression (Figure 4G). Incubation with the PI3K-inhibitors wortmannin (Figure 4H) or Ly294002 (Figure S7) resulted in increased epithelial cell-like morphology and decreased tumor cell scattering.

### **Overexpression of CD63 increased tumor aggressiveness**

As knock down of CD63 provoked a less aggressive tumor cell phenotype, we next evaluated whether CD63 overexpression might exert opposite effects. We overexpressed CD63 (Figure S8A) and assessed the mobility and invasiveness of these cells *in vitro* by evaluation of transwell migration and matrigel invasion (Figure S8B), which were increased. Metastatic properties of these cells were further tested *in vivo* by tail vein inoculation and subsequent analysis of the tumor burden. Upon CD63 overexpression, tumor cell homing (Figure 5A) and metastatic outgrowth (Figure 5B) were increased *in vivo*, suggesting a pivotal role of CD63 in tumor cell aggressiveness.

### **Discussion**

In this study, we show that CD63 increases the metastatic potential of tumor cells by initiating  $\beta$ -catenin-dependent EMT (Figure 6). Our findings suggest that CD63 impacts on the intrinsic metastatic potential of tumor cells, as lack of CD63 produced decreased metastases, while CD63 overexpression increased tumor cell homing. These observations support the notion of a pro-metastatic role of CD63, which is also in line with clinical studies showing that CD63 is upregulated in tumor cells of cancer patients<sup>12-15</sup>. Also, knock down of CD63 decreased the migratory and invasive behavior of different human and murine tumor cell lines. In addition,

MMP-2 and PAI-1, which are both involved in promotion of tumor cell aggressiveness<sup>37</sup> and tissue remodeling initiated by tumor cells<sup>33</sup>, are down-regulated upon CD63 knock down. These findings are in contrast to earlier reports which suggest a tumor-suppressive role of CD63<sup>17-19</sup>, which studied the effect of human CD63 in KM3 cells<sup>19</sup>. However, in our study, we focused on experimental metastasis and the importance of cell plasticity for the metastatic potential. CD63 might differ in its role during other steps of cancer progression which have been described before<sup>17-19</sup>. Our finding that CD63 impacts on EMT and promotes the respective signaling are in line with the role of EMT during metastatic progression: While a mesenchymal cell-like phenotype is of importance in tumor formation<sup>2</sup>, establishment, and initial tumor cell dissemination, tumor cells often convert back to a more epithelial cell-like phenotype at the target site of metastasis<sup>5,38,39</sup>. The ability of individual tumor cells to outgrow and form micro- and subsequently macrometastases at the secondary site is a limiting step during cancer progression, relying on an intrinsic metastatic potential of the tumor cell<sup>40,41</sup>. Tumor cells with intrinsic clonogenic capabilities have been termed cancer stem cells<sup>42</sup>. We suggest that the presence of CD63 is needed for the manifestation of these traits as knock down of CD63 diminished colony formation capability *in vitro* as well as at the site of metastasis by influencing  $\beta$ -catenin levels. CD63 has already been shown to be involved in  $\beta$ -catenin regulation by its role as an interaction partner of TIMP-1<sup>23,27</sup>. TIMP-1 binding to CD63 obtained attention in recent years as it offers a possible starting point for TIMP-1-induced cellular signal transduction leading to increased ERK phosphorylation and PI3K/AKT-pathway activity<sup>12,25</sup>. Thereby, CD63 could participate in NOS-signaling<sup>12</sup> and increase anoikis resistance in melanoma cells<sup>25</sup>. In addition, TIMP-1 has also been shown to induce EMT in canine MCDK cells<sup>26</sup>. As the canine equivalent of CD63 has not been described yet, an involvement of CD63 could also not be verified as yet<sup>26</sup>. We here suggest that modulation of CD63 alone, without the regulation by TIMP-1, is already sufficient to trigger signaling pathways reported for the interaction of CD63 and TIMP-1. Availability of

CD63, possibly dependent on TIMP-1, could be one underlying mechanism behind TIMP-1-induced signaling. As TIMP-1 is heavily involved in the maintenance of the proteolytic equilibrium by its role as a broad-spectrum MMP-inhibitor, its inhibition might cause detrimental effects in cancer treatment<sup>37,43</sup>. In contrast, CD63 might be a valuable target as inhibitory antibodies have already been described<sup>44,45</sup>. In addition to TIMP-1, CD63 can interact with many other proteins which may act as possible downstream effectors of the here described cell signaling pathway. CD63 is a member of the tetraspanin web<sup>16</sup> in which membrane proteins are closely clustered together and form lipid rafts which act as hotspots in cell signaling transduction<sup>16</sup>. Association of tetraspanins with integrins is well-described for these microdomains<sup>8</sup> (Figure S9) and CD63-dependent focal adhesion kinase (FAK)-signaling<sup>16</sup> is reported. Furthermore, CD63 has also been described to interact with the Src family kinases Lyn and Hck<sup>46</sup>, phosphatidylinositol 4-kinase<sup>16</sup>, and members of the AP family<sup>47</sup>. CD63 is also regulated in its localization by Syntenin and L6-antigen-regulated transport mechanisms<sup>16</sup> and regulation of the localization of CD63 could contribute to the signaling pathway we suggest here. In addition, CD63 is involved in the trafficking of different membrane proteins, for example CXCR4<sup>48</sup> and MHCII<sup>49</sup>. Therefore it is also possible that CD63 knock down leads to incorrect processing of a second protein which in turn results in the here described effect, suggesting an indirect role of CD63 in cell signaling. While the identification of the exact interaction partners which are responsible for the CD63-dependent cellular signaling is still ongoing, we here showed here that regulation of CD63 levels already accounts for decisive effects on metastatic success. In summary, the data of the present study give emphasis to the important role of CD63 for metastatic success of tumor cells due to its ability to influence stem cell-like properties of tumor cells and to regulate cell plasticity.

### Acknowledgements

We thank Susanne Schaten and Steve Oswald for expert technical assistance. We acknowledge the excellent support of the Nice-Sophia Antipolis Functional Genomics Platform. We thank Barbara Grünwald for discussion. For financial support, the authors acknowledge the support by grants from the Deutsche Forschungsgemeinschaft (KR2047 1-2, KR2047 3-1 both to AK), the European Union and the Seventh Framework Programme (FP7/2007-2013) under grant agreement n° 263307 (to AK and BM).

Accepted Article

## References

1. Hanahan D, Weinberg RA. Hallmarks of Cancer: The Next Generation. *Cell* 2011;144:646–74.
2. Thiery JP. Epithelial-mesenchymal transitions in tumour progression. *Nat Rev Cancer* 2002;2:442–54.
3. Thiery JP, Acloque H, Huang RYJ, Nieto MA. Epithelial-mesenchymal transitions in development and disease. *Cell* 2009;139:871–90.
4. Kalluri R, Weinberg RA. The basics of epithelial-mesenchymal transition. *Journal of Clinical Investigation* 2009;119:1420–8.
5. Brabletz T. To differentiate or not--routes towards metastasis. *Nat Rev Cancer* 2012;12:425–36.
6. Korpala M, Lee ES, Hu G, Kang Y. The miR-200 Family Inhibits Epithelial-Mesenchymal Transition and Cancer Cell Migration by Direct Targeting of E-cadherin Transcriptional Repressors ZEB1 and ZEB2. *J Biol Chem* 2008;283:14910–4.
7. Kimelman D, Xu W.  $\beta$ -Catenin destruction complex: insights and questions from a structural perspective. *Oncogene* 2006;25:7482–91.
8. Zöller M. Tetraspanins: push and pull in suppressing and promoting metastasis. *Nat Rev Cancer* 2009;9:40–55.
9. Hemler ME. Tetraspanin functions and associated microdomains. *Nat Rev Mol Cell Biol* 2005;6:801–11.
10. Levy S, Shoham T. Protein-protein interactions in the tetraspanin web. *Physiology (Bethesda)* 2005;20:218–24.
11. André M, Le Caer J-P, Greco C, Planchon S, El Nemer W, Boucheix C, Rubinstein E, Chamot-Rooke J, Le Naour F. Proteomic analysis of the tetraspanin web using LC-ESI-MS/MS and MALDI-FTICR-MS. *Proteomics* 2006;6:1437–49.
12. Ridnour LA, Barasch KM, Windhausen AN, Dorsey TH, Lizardo MM, Yfantis HG, Lee DH, Switzer CH, Cheng RYS, Heinecke JL, Brueggemann E, Hines HB, et al. Nitric oxide synthase and breast cancer: role of TIMP-1 in NO-mediated Akt activation. *PLoS ONE* 2012;7:e44081.
13. Rorive S, Lopez XM, Maris C, Trepant A-L, Sauvage S, Sadeghi N, Roland I, Decaestecker C, Salmon I. TIMP-4 and CD63: new prognostic biomarkers in human astrocytomas. *Mod Pathol* 2010;23:1418–28.
14. Lewis TB, Robison JE, Bastien R, Milash B, Boucher K, Samlowski WE, Leachman SA, Dirk Noyes R, Wittwer CT, Perreard L, Bernard PS. Molecular classification of melanoma using real-time quantitative reverse transcriptase-polymerase chain reaction. *Cancer* 2005;104:1678–86.
15. Logozzi M, De Milito A, Lugini L, Borghi M, Calabrò L, Spada M, Perdicchio M, Marino ML, Federici C, Iessi E, Brambilla D, Venturi G, et al. High levels of exosomes

- expressing CD63 and caveolin-1 in plasma of melanoma patients. *PLoS ONE* 2009;4:e5219.
16. Pols MS, Klumperman J. Trafficking and function of the tetraspanin CD63. *Exp Cell Res* 2009;315:1584–92.
  17. Radford KJ, Mallesch J, Hersey P. Suppression of human melanoma cell growth and metastasis by the melanoma-associated antigen CD63 (ME491). *Int J Cancer* 1995;62:631–5.
  18. Radford KJ, Thorne RF, Hersey P. CD63 associates with transmembrane 4 superfamily members, CD9 and CD81, and with beta 1 integrins in human melanoma. *Biochem Biophys Res Commun* 1996;222:13–8.
  19. Radford KJ, Thorne RF, Hersey P. Regulation of tumor cell motility and migration by CD63 in a human melanoma cell line. *J Immunol* 1997;158:3353–8.
  20. Jang H-I, Lee H. A decrease in the expression of CD63 tetraspanin protein elevates invasive potential of human melanoma cells. *Exp Mol Med* 2003;35:317–23.
  21. Kwon MS, Shin S-H, Yim S-H, Lee KY, Kang H-M, Kim T-M, Chung Y-J. CD63 as a biomarker for predicting the clinical outcomes in adenocarcinoma of lung. *Lung Cancer* 2007;57:46–53.
  22. Zhijun X, Shulan Z, Zhuo Z. Expression and significance of the protein and mRNA of metastasis suppressor gene ME491/CD63 and integrin alpha5 in ovarian cancer tissues. *Eur J Gynaecol Oncol* 2007;28:179–83.
  23. Jung K-K, Liu X-W, Chirco R, Fridman R, Kim H-RC. Identification of CD63 as a tissue inhibitor of metalloproteinase-1 interacting cell surface protein. *EMBO J* 2006;25:3934–42.
  24. Cruz-Munoz W, Khokha R. The role of tissue inhibitors of metalloproteinases in tumorigenesis and metastasis. *Crit Rev Clin Lab Sci* 2008;45:291–338.
  25. Toricelli M, Melo FH, Peres GB, Silva DC, Jasiulionis MG. Timp1 interacts with beta-1 integrin and CD63 along melanoma genesis and confers anoikis resistance by activating PI3-K signaling pathway independently of Akt phosphorylation. *Molecular Cancer* 2013;12:22.
  26. Jung YS, Liu X-W, Chirco R, Warner RB, Fridman R, Kim H-RC. TIMP-1 Induces an EMT-Like Phenotypic Conversion in MDCK Cells Independent of Its MMP-Inhibitory Domain. *PLoS ONE* 2012;7:e38773.
  27. Egea V, Zahler S, Rieth N, Neth P, Popp T, Kehe K, Jochum M, Ries C. Tissue inhibitor of metalloproteinase-1 (TIMP-1) regulates mesenchymal stem cells through let-7f microRNA and Wnt/ $\beta$ -catenin signaling. *Proc Natl Acad Sci USA* 2012;109:E309–16.
  28. Hauser S, Bickel L, Weinspach D, Gerg M, Schäfer MK, Pfeifer M, Hazin J, Schelter F, Weidle UH, Ramser J, Volkmann J, Meindl A, et al. Full-length LICAM and not its  $\Delta 2\Delta 27$  splice variant promotes metastasis through induction of gelatinase expression. *PLoS ONE* 2011;6:e18989.

29. Schelter F, Kobuch J, Moss ML, Becherer JD, Comoglio PM, Boccaccio C, Krüger A. A disintegrin and metalloproteinase-10 (ADAM-10) mediates DN30 antibody-induced shedding of the met surface receptor. *J Biol Chem* 2010;285:26335–40.
30. Schambach A, Mueller D, Galla M, Verstegen MMA, Wagemaker G, Loew R, Baum C, Bohne J. Overcoming promoter competition in packaging cells improves production of self-inactivating retroviral vectors. *Gene Ther* 2006;13:1524–33.
31. Dumas JE, Platt MO. Systematic optimization of multiplex zymography protocol to detect active cathepsins K, L, S, and V in healthy and diseased tissue: compromise between limits of detection, reduced time, and resources. *Mol Biotechnol* 2013;54:1038–47.
32. Krüger A, Soeltl R, Sopov I, Kopitz C, Arlt M, Magdolen V, Harbeck N, Gänsbacher B, Schmitt M. Hydroxamate-Type Matrix Metalloproteinase Inhibitor Batimastat Promotes Liver Metastasis. *Cancer Res* 2001;61:1272–5.
33. He W, Tan R, Dai C, Li Y, Wang D, Hao S, Kahn M, Liu Y. Plasminogen Activator Inhibitor-1 Is a Transcriptional Target of the Canonical Pathway of Wnt/ $\beta$ -Catenin Signaling. *J Biol Chem* 2010;285:24665–75.
34. Doyle JL, Haas TL. Differential role of  $\beta$ -catenin in VEGF and histamine-induced MMP-2 production in microvascular endothelial cells. *J Cell Biochem* 2009;107:272–83.
35. Cross DA, Alessi DR, Cohen P, Andjelkovich M, Hemmings BA. Inhibition of glycogen synthase kinase-3 by insulin mediated by protein kinase B. *Nature* 1995;378:785–9.
36. Zavadil J, Böttinger EP. TGF- $\beta$  and epithelial-to-mesenchymal transitions. *Oncogene* 2005;24:5764–74.
37. Krüger A. Functional genetic mouse models: promising tools for investigation of the proteolytic internet. *Biol Chem* 2009;390:91–7.
38. Tsai JH, Donaher JL, Murphy DA, Chau S, Yang J. Spatiotemporal regulation of epithelial-mesenchymal transition is essential for squamous cell carcinoma metastasis. *Cancer Cell* 2012;22:725–36.
39. Ocaña OH, Córcoles R, Fabra A, Moreno-Bueno G, Acloque H, Vega S, Barrallo-Gimeno A, Cano A, Nieto MA. Metastatic colonization requires the repression of the epithelial-mesenchymal transition inducer Prrx1. *Cancer Cell* 2012;22:709–24.
40. Chambers AF, Groom AC, MacDonald IC. Dissemination and growth of cancer cells in metastatic sites. *Nat Rev Cancer* 2002;2:563–72.
41. Nguyen DX, Bos PD, Massagué J. Metastasis: from dissemination to organ-specific colonization. *Nat Rev Cancer* 2009;9:274–84.
42. Dalerba P, Clarke MF. Cancer stem cells and tumor metastasis: first steps into uncharted territory. *Cell Stem Cell* 2007;1:241–2.
43. Overall CM, Dean RA. Degradomics: systems biology of the protease web. Pleiotropic roles of MMPs in cancer. *Cancer Metastasis Rev* 2006;25:69–75.

44. Sordat I, Decraene C, Silvestre T, Petermann O, Auffray C, Piétu G, Sordat B. Complementary DNA arrays identify CD63 tetraspanin and alpha3 integrin chain as differentially expressed in low and high metastatic human colon carcinoma cells. *Lab Invest* 2002;82:1715–24.
45. Mantegazza AR, Barrio MM, Moutel S, Bover L, Weck M, Brossart P, Teillaud J-L, Mordoh J. CD63 tetraspanin slows down cell migration and translocates to the endosomal-lysosomal-MIICs route after extracellular stimuli in human immature dendritic cells. *Blood* 2004;104:1183–90.
46. Skubitz KM, Campbell KD, Iida J, Skubitz AP. CD63 associates with tyrosine kinase activity and CD11/CD18, and transmits an activation signal in neutrophils. *J Immunol* 1996;157:3617–26.
47. Rous BA, Reaves BJ, Ihrke G, Briggs JAG, Gray SR, Stephens DJ, Banting G, Luzio JP. Role of Adaptor Complex AP-3 in Targeting Wild-Type and Mutated CD63 to Lysosomes. *Mol Biol Cell* 2002;13:1071–82.
48. Yoshida N, Kitayama D, Arima M, Sakamoto A, Inamine A, Watanabe-Takano H, Hatano M, Koike T, Tokuhisa T. CXCR4 expression on activated B cells is downregulated by CD63 and IL-21. *J Immunol* 2011;186:2800–8.
49. Petersen SH, Odintsova E, Haigh TA, Rickinson AB, Taylor GS, Berditchevski F. The role of tetraspanin CD63 in antigen presentation via MHC class II. *Eur J Immunol* 2011;41:2556–61.

## Figure legends

### Figure 1: Knock down of CD63 decreased tumor cell homing, metastatic outgrowth and clonogenic capacity.

(A-C)  $1 \times 10^6$  SKOV3ipL (A, C) or  $2 \times 10^5$  B16F10L (C) cells were intravenously inoculated into NMRI<sup>nu/nu</sup> (A, C) or C57Bl/6 (B) mice and sacrificed at the indicated time point. Organs were stained using X-Gal to visualize *lacZ*-tagged tumor cells.

(A) CD63 knock down reduced outgrowth of SKOV3ipL cells. Representative overview (upper panel; Bar, 2 mm) and close-up (lower panel; Bar, 0.5 mm) pictures of the lung (left)

and quantification of tumor cells. (B) CD63 knock down reduced outgrowth of B16F10L cells. Representative overview (upper panel; Bar, 5 mm) and close-up (lower panel; Bar, 0.5 mm) pictures of the lung and quantification of tumor cells.

(C) CD63 knock down reduced tumor cell homing of SKOV3ipL cells. Representative overview (upper panel; Bar, 2 mm) and close-up (lower panel; Bar, 0.5 mm) pictures of the lung (left) and quantification of tumor cells.

(D) Clonogenic assay using SKOV3ipL cells show decreased resistance against cisplatin, if CD63 is knocked down. Representative pictures (left panel). Bar, 1 cm. (A, B)

*lacZ* mRNA is shown relative to 18S rRNA and normalized to the respective control (empty).

(A-D): Results are shown as mean  $\pm$  SEM (error bars). \*P  $\leq$  0.05; \*\*P  $\leq$  0.01; \*\*\*P  $\leq$  0.01;

\*\*\*\*P  $\leq$  0.0001; unpaired *t* test. (n = 5). *shNT*: cell lines stably transduced with non-target

shRNA control. *shCD63*: cell lines stably transduced with shRNA against CD63.

### Figure 2: Knock down of CD63 decreases $\beta$ -catenin activity and increases active GSK3 $\beta$ levels.

(A-C)  $\beta$ -catenin levels are reduced on protein level upon CD63 knock down.

Quantification of  $\beta$ -catenin (*CTNNB1*) on mRNA (A) and protein level (B and C) using qRT-PCR (A), Western blot (B), or ICC (C), respectively, in SKOV3ipL cells. (D, E)  $\beta$ -catenin

targets PAI-1 and MMP-2 are reduced upon CD63 knock down in SKOV3ipL cells.

Quantification of the direct  $\beta$ -catenin transcriptional target PAI-1 (D) or MMP-2 (E) on

mRNA levels was done using qRT-PCR. (F) CD63 knock down reduced levels of inactivated, phosphorylated GSK3 $\beta$ . Estimation of phosphorylated GSK3 $\beta$  levels using Western blot.  $\alpha$ -Tub was used as a loading control. (G) PI3K and AKT levels were quantified using Western blot.  $\alpha$ -Tub was used as a loading control. (A, E, F) Target mRNA is shown relative to 18S rRNA and normalized to the respective control (*shNT*). Results are mean  $\pm$  SEM (*error bars*)  $n = 3$ . \*\*\* $P \leq 0.001$ , unpaired *t* test. (A-G) *shNT*: cell lines stably transduced with non-target shRNA control. *shCD63*: cell lines stably transduced with shRNA against CD63.

**Figure 3: CD63 is important for maintenance of a mesenchymal-like, aggressive tumor cell phenotype.** (A, B) CD63 knock down changes cell morphology in SKOV3ipL (A) and B16F10L (B) cells. Cells were analyzed for the shape of the colonies and divided into scattered and non-scattered phenotypes (exemplary DIC pictures on the left side). (C, D) Epithelial marker E-cadherin levels are increased upon CD63 knock down in SKOV3ipL (C) and B16F10 (D) cells. E-cadherin (*CDH1*) was quantified on mRNA level using qRT-PCR (C, D) and on protein level using Western blot (D).  $\alpha$ -Tub was used as a loading control. (E, F) Mesenchymal marker N-cadherin (*CDH2*) levels are reduced upon CD63 knock down in SKOV3ipL (E) and B16F10 (F) cells. N-cadherin was quantified on mRNA level using qRT-PCR (E, F) and on protein level using Western blot.  $\alpha$ -Tub was used as a loading control. (E) (G, H) E-cadherin repressors SLUG (G) and ZEB1 (H) are reduced upon CD63 knock down. Protein levels were quantified using Western blot,  $\alpha$ -Tub was used as a loading control. (I) miR-141 levels are increased upon CD63 knock down. miR-141 was quantified using qRT-PCR. (J) CD63 knock down reduced cell migration and invasion *in vitro*. Cell migration and matrigel invasion were assessed using transwell assays. (C-E, I): Target mRNA is shown relative to 18S rRNA, or U6 snRNA (I), respectively, and normalized to the respective control (*shNT*). (A-F, I, J): Results are shown as mean  $\pm$  SEM (*error bars*). \* $P \leq 0.05$ ; \*\* $P \leq 0.01$ ; \*\*\* $P \leq 0.01$ ; \*\*\*\* $P \leq 0.0001$ ; unpaired *t* test. ( $n = 3$ ). (A-J): *shNT*: cell lines stably transduced

with non-target shRNA control. *shCD63*: cell lines stably transduced with shRNA against CD63.

**Figure 4: Blockage of CD63-dependent effects using downstream target inhibitors**

(A-C): Knock down of CD63 renders cells resistant to TGF- $\beta$ 1-induced cell scattering and induction of  $\beta$ -catenin targets by TGF- $\beta$ 1. (A): SKOV3ipL cells were incubated with TGF- $\beta$ 1 and cell colony shape was evaluated. mRNA levels of  $\beta$ -catenin target genes *Pail1* (B) and *MMP2* (C) were evaluated using qRT-PCR. (D, E): Inhibition of  $\beta$ -catenin using quercetin mimics CD63 knock down effects. (D): SKOV3ipL cells were incubated with quercetin and cell colony shape was evaluated. (E): mRNA levels of epithelial cell marker E-cadherin (*CDH1*) was evaluated using qRT-PCR. (F, G): Inhibition of GSK3 $\beta$  using SB216763 reduced CD63 knock down effects. (F): SKOV3ipL cells were incubated with SB216763 and cell colony shape was evaluated. (G): mRNA levels of epithelial cell marker E-cadherin (*CDH1*) was evaluated using qRT-PCR. (H): Inhibition of PI3K mimics CD63 knock down. SKOV3ipL cells were incubated with wortmannin and cell colony shape was evaluated. (B, C, F, E) Target mRNA is shown relative to 18S rRNA and normalized to the respective control (*shNT*). (A-E, G) Results are shown as mean  $\pm$  SEM (*error bars*). \* $P \leq 0.05$ ; \*\* $P \leq 0.01$  (n = 3). (A-H): *shNT*: cell lines stably transduced with non-target shRNA control. *shCD63*: cell lines stably transduced with shRNA against CD63.

**Figure 5: CD63 overexpression increases the tumor cell-intrinsic metastatic potential.**

(A, B)  $1 \times 10^6$  SKOV3ipL cells were intravenously inoculated in NMRI<sup>nu/nu</sup> mice and sacrificed 24 hours (A) or 35 days (B) after tumor cell inoculation, respectively. Organs were stained using X-Gal to visualize *lacZ*-tagged tumor cells. CD63 overexpression increased tumor cell homing of SKOV3ipL cells. Representative overview (upper panel; *Bar*, 2 mm) and close-up (lower panel; *Bar*, 0.5 mm) pictures of the lung (left) and quantification of tumor

cells using *lacZ*-qRT-PCR. *empty*: cell lines stably transduced with empty control vector. *CD63<sup>high</sup>*: cell lines stably transduced for CD63 overexpression.

**Figure 6: CD63 induced EMT via  $\beta$ -catenin and CD63 levels determine the cellular phenotype**

Left side: Proposed pathway of CD63-dependent signaling. <sup>1</sup>Involvement of PI3K was shown using the PI3K-inhibitors wortmannin and Ly294002. <sup>2</sup>Involvement of GSK3 $\beta$  was shown using the inhibitor *SB-216763*. <sup>3</sup>Involvement of  $\beta$ -catenin was shown using the inhibitor quercetin. Right side: Summary of phenotypical changes upon CD63 knock down.

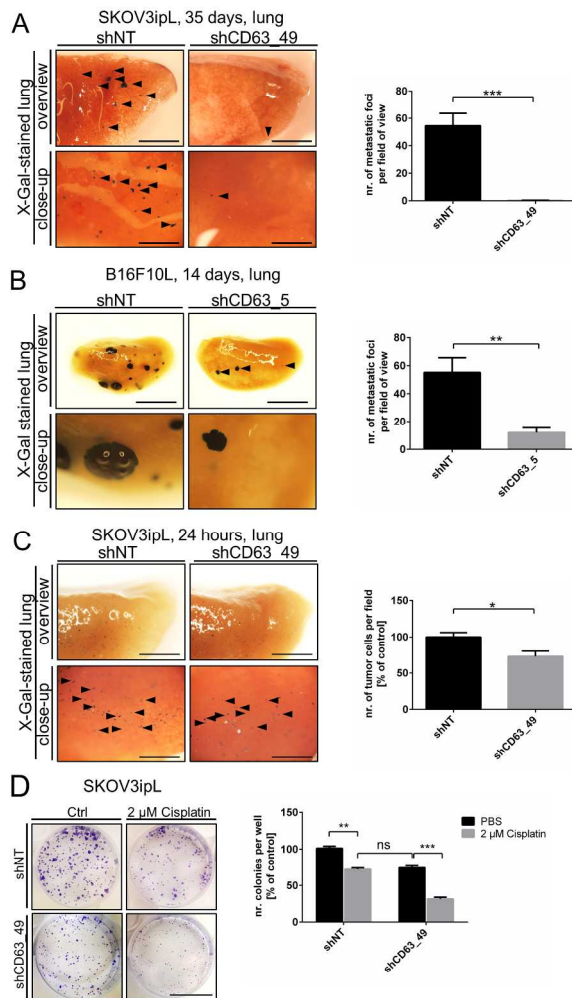


Figure 1: Knock down of CD63 decreased tumor cell homing, metastatic outgrowth and clonogenic capacity. (A-C)  $1 \times 10^6$  SKOV3ipL (A, C) or  $2 \times 10^5$  B16F10L (C) cells were intravenously inoculated into NMRInu/nu (A, C) or C57Bl/6 (B) mice and sacrificed at the indicated time point. Organs were stained using X-Gal to visualize lacZ-tagged tumor cells. (A) CD63 knock down reduced outgrowth of SKOV3ipL cells. Representative overview (upper panel; Bar, 2 mm) and close-up (lower panel; Bar, 0.5 mm) pictures of the lung (left) and quantification of tumor cells. (B) CD63 knock down reduced outgrowth of B16F10L cells. Representative overview (upper panel; Bar, 5 mm) and close-up (lower panel; Bar, 0.5 mm) pictures of the lung and quantification of tumor cells. (C) CD63 knock down reduced tumor cell homing of SKOV3ipL cells. Representative overview (upper panel; Bar, 2 mm) and close-up (lower panel; Bar, 0.5 mm) pictures of the lung (left) and quantification of tumor cells. (D) Clonogenic assay using SKOV3ipL cells show decreased resistance against cisplatin, if CD63 is knocked down. Representative pictures (left panel). Bar, 1 cm. (A, B) lacZ mRNA is shown relative to 18S rRNA and normalized to the respective control (empty). (A-D): Results are shown as mean  $\pm$  SEM (error bars). \* $P \leq 0.05$ ; \*\* $P \leq 0.01$ ; \*\*\* $P \leq 0.01$ ; \*\*\*\* $P \leq 0.0001$ ; unpaired t

test. (n = 5). shNT: cell lines stably transduced with non-target shRNA control. shCD63: cell lines stably transduced with shRNA against CD63.

190x254mm (300 x 300 DPI)

Accepted Article

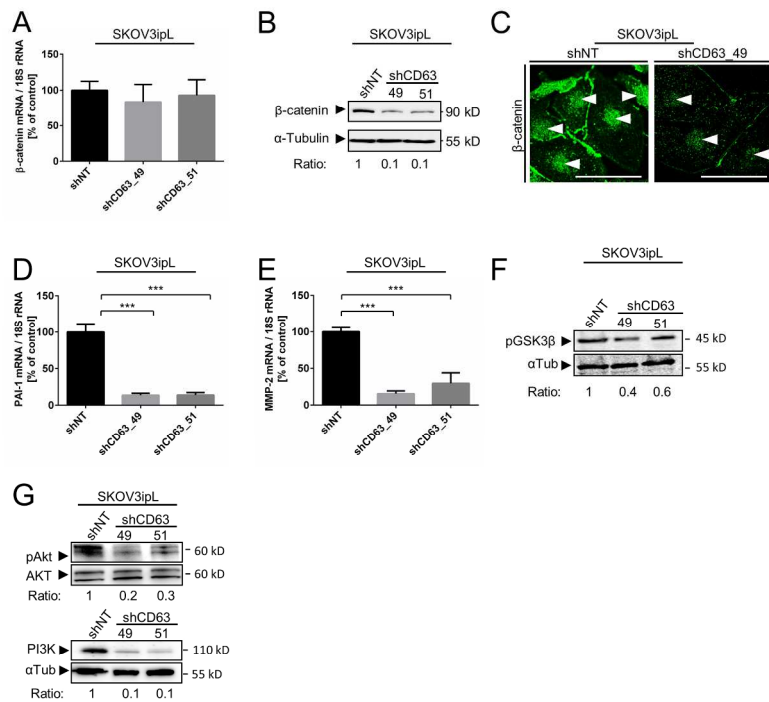


Figure 2: Knock down of CD63 decreases  $\beta$ -catenin activity and increases active GSK3 $\beta$  levels. (A-C)  $\beta$ -catenin levels are reduced on protein level upon CD63 knock down. Quantification of  $\beta$ -catenin (CTNNB1) on mRNA (A) and protein level (B and C) using qRT-PCR (A), Western blot (B), or ICC (C), respectively, in SKOV3ipL cells. (D, E)  $\beta$ -catenin targets PAI-1 and MMP-2 are reduced upon CD63 knock down in SKOV3ipL cells. Quantification of the direct  $\beta$ -catenin transcriptional target PAI-1 (D) or MMP-2 (E) on mRNA levels was done using qRT-PCR. (F) CD63 knock down reduced levels of inactivated, phosphorylated GSK3 $\beta$ . Estimation of phosphorylated GSK3 $\beta$  levels using Western blot.  $\alpha$ -Tub was used as a loading control. (G) PI3K and AKT levels were quantified using Western blot.  $\alpha$ -Tub was used as a loading control. (A, E, F) Target mRNA is shown relative to 18S rRNA and normalized to the respective control (shNT). Results are mean  $\pm$  SEM (error bars)  $n = 3$ . \*\*\* $P \leq 0.001$ , unpaired t test. (A-G) shNT: cell lines stably transduced with non-target shRNA control. shCD63: cell lines stably transduced with shRNA against CD63.

190x254mm (300 x 300 DPI)

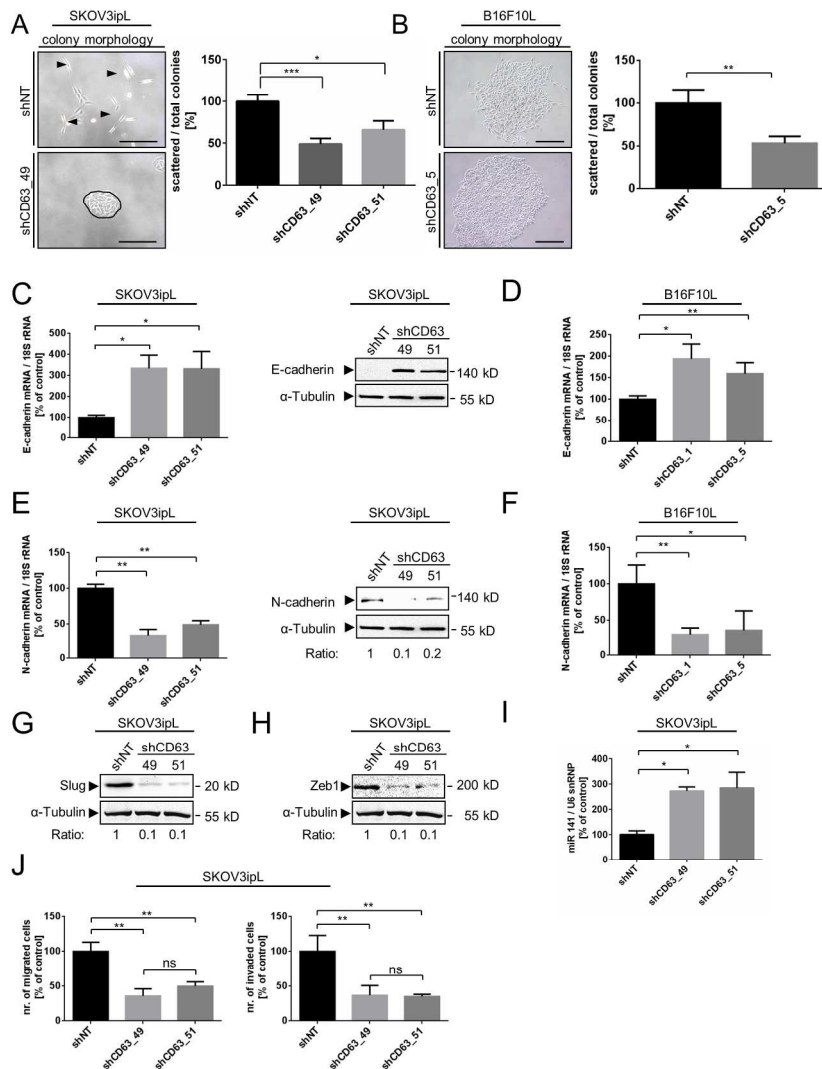


Figure 3: CD63 is important for maintenance of a mesenchymal-like, aggressive tumor cell phenotype. (A, B) CD63 knock down changes cell morphology in SKOV3ipL (A) and B16F10L (B) cells. Cells were analyzed for the shape of the colonies and divided into scattered and non-scattered phenotypes (exemplary DIC pictures on the left side). (C, D) Epithelial marker E-cadherin levels are increased upon CD63 knock down in SKOV3ipL (C) and B16F10L (D) cells. E-cadherin (CDH1) was quantified on mRNA level using qRT-PCR (C, D) and on protein level using Western blot (D).  $\alpha$ -Tub was used as a loading control. (E, F) Mesenchymal marker N-cadherin (CDH2) levels are reduced upon CD63 knock down in SKOV3ipL (E) and B16F10L (F) cells. N-cadherin was quantified on mRNA level using qRT-PCR (E, F) and on protein level using Western blot.  $\alpha$ -Tub was used as a loading control. (E) (G, H) E-cadherin repressors SLUG (G) and ZEB1 (H) are reduced upon CD63 knock down. Protein levels were quantified using Western blot,  $\alpha$ -Tub was used as a loading control. (I) miR-141 levels are increased upon CD63 knock down. miR-141 was quantified using qRT-PCR. (J) CD63 knock down reduced cell migration and invasion in vitro. Cell migration and matrigel invasion were assessed using transwell assays. (C-E, I): Target mRNA is shown relative to 18S rRNA, or U6 snRNA (I),

respectively, and normalized to the respective control (shNT). (A-F, I, J): Results are shown as mean  $\pm$  SEM (error bars). \*P  $\leq$  0.05; \*\*P  $\leq$  0.01; \*\*\*P  $\leq$  0.001; \*\*\*\*P  $\leq$  0.0001; unpaired t test. (n = 3). (A-J): shNT: cell lines stably transduced with non-target shRNA control. shCD63: cell lines stably transduced with shRNA against CD63.

190x254mm (300 x 300 DPI)

Accepted Article

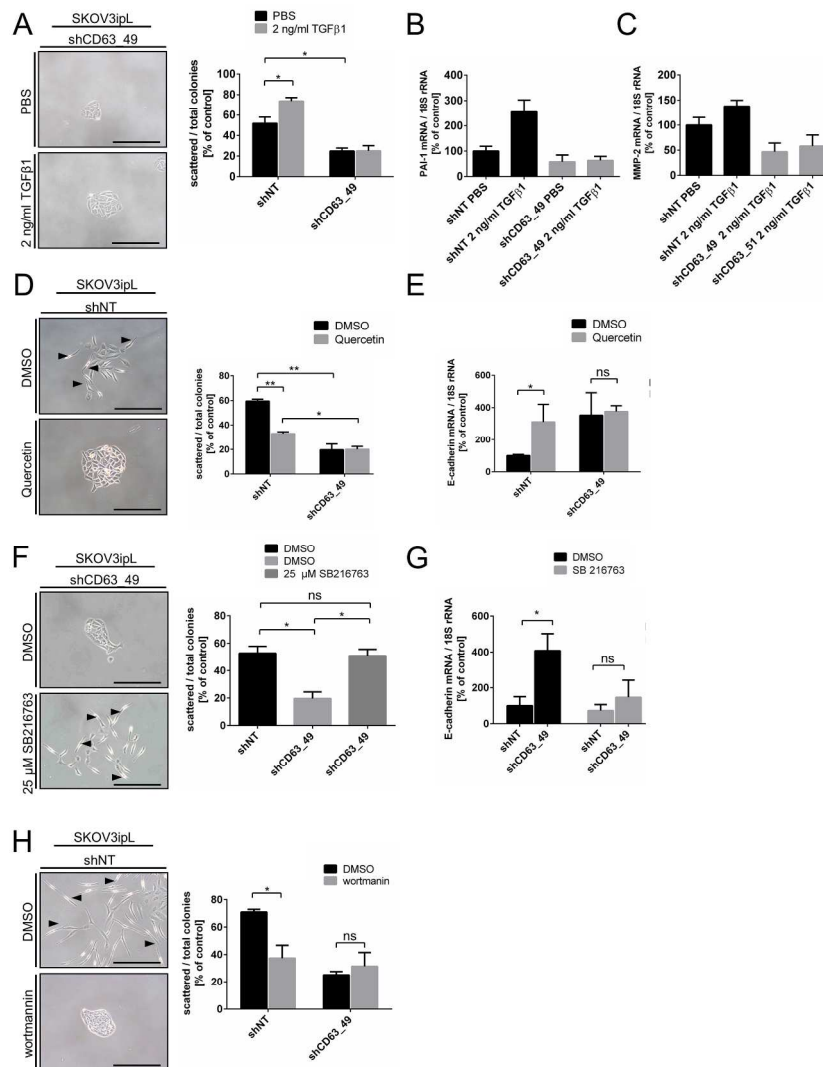


Figure 4: Blockage of CD63-dependent effects using downstream target inhibitors

(A-C): Knock down of CD63 renders cells resistant to TGF-β1-induced cell scattering and induction of β-catenin targets by TGF-β1. (A): SKOV3ipL cells were incubated with TGF-β1 and cell colony shape was evaluated. mRNA levels of β-catenin target genes PAI1 (B) and MMP2 (C) were evaluated using qRT-PCR. (D, E): Inhibition of β-catenin using quercetin mimics CD63 knock down effects. (D): SKOV3ipL cells were incubated with quercetin and cell colony shape was evaluated. (E): mRNA levels of epithelial cell marker E-cadherin (CDH1) was evaluated using qRT-PCR. (F, G): Inhibition of GSK3β using SB216763 reduced CD63 knock down effects. (F): SKOV3ipL cells were incubated with SB216763 and cell colony shape was evaluated. (G): mRNA levels of epithelial cell marker E-cadherin (CDH1) was evaluated using qRT-PCR. (H): Inhibition of PI3K mimics CD63 knock down. SKOV3ipL cells were incubated with wortmannin and cell colony shape was evaluated. (B, C, F, E) Target mRNA is shown relative to 18S rRNA and normalized to the respective control (shNT). (A-E, G) Results are shown as mean ± SEM (error bars). \*P ≤ 0.05; \*\*P ≤ 0.01 (n = 3). (A-H): shNT: cell lines stably transduced with non-target shRNA control. shCD63: cell lines stably

Accepted Article

transduced with shRNA against CD63.

190x254mm (300 x 300 DPI)

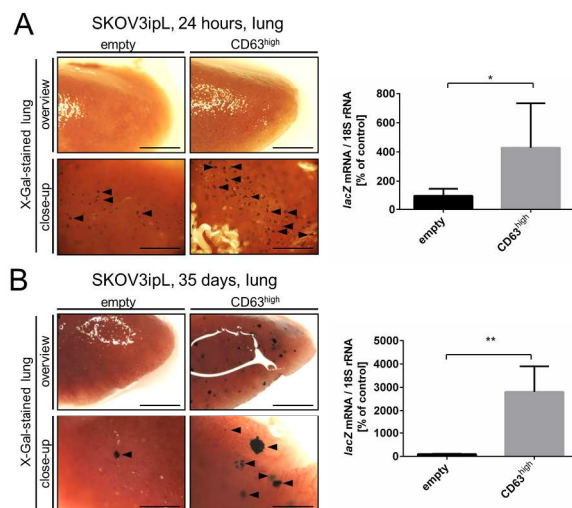


Figure 5: CD63 overexpression increases the tumor cell-intrinsic metastatic potential. (A, B)  $1 \times 10^6$  SKOV3ipL cells were intravenously inoculated in NMRInu/nu mice and sacrificed 24 hours (A) or 35 days (B) after tumor cell inoculation, respectively. Organs were stained using X-Gal to visualize lacZ-tagged tumor cells. CD63 overexpression increased tumor cell homing of SKOV3ipL cells. Representative overview (upper panel; Bar, 2 mm) and close-up (lower panel; Bar, 0.5 mm) pictures of the lung (left) and quantification of tumor cells using lacZ-qRT-PCR. empty: cell lines stably transduced with empty control vector. CD63<sup>high</sup>: cell lines stably transduced for CD63 overexpression.

190x254mm (300 x 300 DPI)

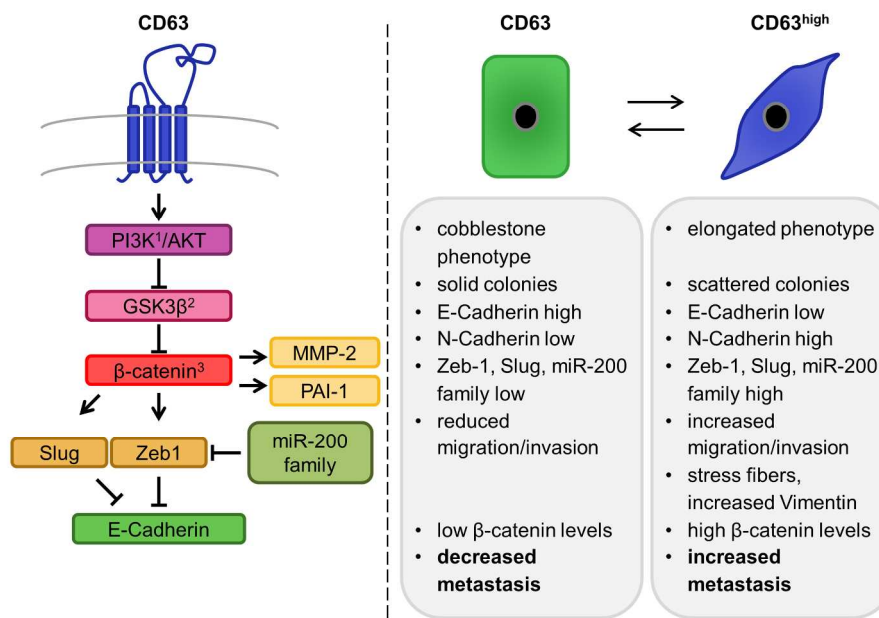


Figure 6: CD63 induced EMT via  $\beta$ -catenin and CD63 levels determine the cellular phenotype  
 Left side: Proposed pathway of CD63-dependent signaling. 1Involvement of PI3K was shown using the PI3K-inhibitors wortmannin and Ly294002. 2Involvement of GSK3 $\beta$  was shown using the inhibitor SB-216763. 3Involvement of  $\beta$ -catenin was shown using the inhibitor quercetin. Right side: Summary of phenotypical changes upon CD63 knock down.

190x254mm (300 x 300 DPI)

A

Table S1. Analyses of deregulated “Diseases and Functions” according to Ingenuity Pathway Analysis of microarray datasets from CD63 knock down in SKOV3ipL cells. shCD63\_49: SKOV3ipL shCD63\_49, shCD63\_51: SKOV3ipL shCD63\_51. The Z-score in each category is represented.

<b>Diseases and Bio Functions</b>	<b>shCD63_49 vs shNT</b>	<b>shCD63_51 vs shNT</b>
cell movement of tumor cell lines	-1.92	-2.02
invasion of tumor cell lines	0.46	-2.04
colony formation of cells	0.21	-1.98
organismal death	-2.63	-0.41
concentration of lipid	-2.95	
colony formation of tumor cell lines	-0.52	-1.36
nodule	-1.41	0.00
development of head	-1.29	0.00
development of body axis	-1.29	0.00
cell movement	-1.43	-0.79
inflammation of organ	-1.33	-0.34
recruitment of cells	-1.21	-0.54
migration of cells	-1.32	-0.49
necrosis	-1.80	0.33
quantity of filaments	-2.41	
infection of mammalia	-2.25	
metabolism of terpenoid	-2.11	
remodeling of blood vessel	-2.00	
congenital urogenital anomaly	-2.00	
development of digestive system	-1.98	
concentration of cholesterol	-1.99	
Thrombosis	-1.99	
cell death	-1.30	0.67
quantity of gonadal cells	-1.38	

Table S2. List of selected protease expressions from the comparison of transcriptome from SKOV3ipL cell lines. Logarithm (base 2) of the average intensity and logarithm (base 2) of the ratio (shCD63 vs shNT) as well as corresponding adjusted p-values are represented. A: Mean expression of intensity. M: Mean ratio shCD63 vs. shNT. P-Val: p-values. TRUE/FALSE: Last two columns represent if the modulation of certain gene is significant („True“) concerning cut off values of A>6, absolute value of M> 0,7 and pVal< 0,05. „False“

Gene Name	A	M shCD63_49	PVal shCD63_49	M shCD63_51	PVal shCD63_51	shCD63-49	shCD63-51
MMP1	11.64	1.19	4.28E-02	0.80	3.38E-01	TRUE	FALSE
MMP2	5.68	-0.33	6.93E-01	-0.38	8.00E-01	FALSE	FALSE
MMP3	4.61	-0.40	7.70E-01	-0.39	8.72E-01	FALSE	FALSE
<b>MMP7</b>	<b>7.78</b>	<b>2.18</b>	<b>3.02E-02</b>	<b>0.83</b>	<b>6.92E-01</b>	<b>TRUE</b>	<b>FALSE</b>
MMP8	4.88	0.13	9.63E-01	0.12	9.76E-01	FALSE	FALSE
MMP9	8.66	-0.06	9.67E-01	0.02	9.96E-01	FALSE	FALSE
MMP10	6.76	1.17	1.34E-01	0.28	9.01E-01	FALSE	FALSE
MMP11	6.37	0.15	9.01E-01	-0.15	9.36E-01	FALSE	FALSE
MMP12	4.68	0.54	6.31E-01	0.20	9.51E-01	FALSE	FALSE
MMP13	4.63	-0.09	9.73E-01	-0.11	9.78E-01	FALSE	FALSE
MMP14	5.05	-0.04	9.85E-01	0.17	9.27E-01	FALSE	FALSE
MMP15	10.69	0.42	5.36E-01	-0.06	9.83E-01	FALSE	FALSE
MMP16	5.33	-0.21	8.18E-01	-0.44	7.25E-01	FALSE	FALSE
MMP17	10.33	0.01	9.99E-01	0.15	9.81E-01	FALSE	FALSE
MMP19	6.82	0.03	9.85E-01	0.02	9.92E-01	FALSE	FALSE
MMP19	8.91	0.33	6.65E-01	0.21	8.97E-01	FALSE	FALSE
MMP20	4.81	0.02	9.91E-01	-0.26	8.29E-01	FALSE	FALSE
MMP21	5.48	0.23	7.60E-01	-0.20	8.86E-01	FALSE	FALSE
MMP23B	5.63	0.32	8.09E-01	0.04	9.93E-01	FALSE	FALSE
MMP24	13.17	-0.11	9.38E-01	-1.45	5.16E-02	FALSE	FALSE
MMP25	5.30	-0.22	8.67E-01	-0.01	9.98E-01	FALSE	FALSE
MMP25	6.89	-0.17	8.36E-01	0.24	8.42E-01	FALSE	FALSE
MMP26	4.61	0.05	9.88E-01	-0.12	9.72E-01	FALSE	FALSE
MMP27	4.92	-0.14	9.10E-01	-0.06	9.79E-01	FALSE	FALSE
MMP28	8.55	-0.06	9.75E-01	0.32	8.28E-01	FALSE	FALSE

represents no significant modulation according to adjusted cut-off values. shCD63\_49: SKOV3ipL shCD63\_49, shCD63\_51: SKOV3ipL shCD63\_51.

Gene Name	A	M shCD63_49	PVal shCD63_49	M shCD63_51	PVal shCD63_51	shCD63-49	shCD63-51
ADAM1	6.61	-0.34	5.52E-01	0.34	7.58E-01	FALSE	FALSE
ADAM2	4.62	0.10	9.68E-01	0.25	9.27E-01	FALSE	FALSE
ADAM3A	4.97	0.49	3.50E-01	0.21	8.72E-01	FALSE	FALSE

ADAM6	4.75	0.84	5.38E-01	-0.12	9.81E-01	FALSE	FALSE
ADAM7	5.30	-0.55	6.03E-01	0.28	9.11E-01	FALSE	FALSE
ADAM8	7.19	0.70	2.99E-01	-0.13	9.59E-01	FALSE	FALSE
ADAM9	6.27	-0.11	9.59E-01	0.08	9.84E-01	FALSE	FALSE
ADAM10	9.99	0.30	6.66E-01	0.15	9.27E-01	FALSE	FALSE
ADAM11	7.78	0.27	6.85E-01	-0.65	3.81E-01	FALSE	FALSE
ADAM11	8.33	-0.51	5.73E-01	-0.27	9.01E-01	FALSE	FALSE
ADAM12	6.77	-0.79	2.69E-01	-0.40	8.14E-01	FALSE	FALSE
ADAM12	6.43	-0.55	3.67E-01	-0.38	7.68E-01	FALSE	FALSE
ADAM12	5.16	-0.29	7.49E-01	-0.35	8.19E-01	FALSE	FALSE
ADAM15	10.85	0.19	9.21E-01	-0.07	9.85E-01	FALSE	FALSE
ADAM15	15.16	0.12	9.02E-01	0.25	8.25E-01	FALSE	FALSE
ADAM17	9.01	-0.08	9.73E-01	0.17	9.59E-01	FALSE	FALSE
ADAM18	4.60	-0.06	9.76E-01	0.44	7.55E-01	FALSE	FALSE
ADAM18	4.78	0.04	9.89E-01	-0.28	8.84E-01	FALSE	FALSE
ADAM19	11.95	-0.77	3.06E-01	0.79	5.43E-01	FALSE	FALSE
ADAM19	5.85	-0.17	9.01E-01	0.72	5.46E-01	FALSE	FALSE
ADAM20	4.82	0.16	9.25E-01	0.24	9.16E-01	FALSE	FALSE
ADAM21	4.80	-0.12	9.39E-01	0.50	7.15E-01	FALSE	FALSE
ADAM21	5.02	-0.11	9.71E-01	0.56	8.07E-01	FALSE	FALSE
ADAM22	6.38	-0.16	9.70E-01	-0.25	9.64E-01	FALSE	FALSE
ADAM23	6.72	-0.54	2.70E-01	-1.62	1.88E-02	TRUE	FALSE
ADAM23	6.49	-0.38	5.22E-01	-0.80	2.36E-01	FALSE	FALSE
ADAM28	5.08	0.01	9.97E-01	-0.17	9.34E-01	FALSE	FALSE
ADAM29	5.10	-0.44	6.28E-01	-0.72	6.03E-01	FALSE	FALSE
ADAM29	5.07	-0.14	9.22E-01	-0.16	9.42E-01	FALSE	FALSE
ADAM29	4.64	0.18	9.49E-01	0.59	8.25E-01	FALSE	FALSE
ADAM30	4.84	0.51	5.11E-01	0.50	7.41E-01	FALSE	FALSE
ADAM32	5.14	0.13	9.23E-01	0.05	9.85E-01	FALSE	FALSE
ADAM32	4.77	0.16	9.30E-01	0.11	9.72E-01	FALSE	FALSE
ADAM33	6.96	-0.08	9.74E-01	0.22	9.28E-01	FALSE	FALSE
ADAM33	5.38	-0.35	6.38E-01	-0.04	9.88E-01	FALSE	FALSE
ADAM33	6.18	0.29	7.42E-01	0.13	9.59E-01	FALSE	FALSE

Gene Name	A	M shCD63_49	PVal shCD63_49	M shCD63_51	PVal shCD63_51	shCD63-49	shCD63-51
ADAMTS1	9.70	-1.83	1.31E-02	-1.18	1.41E-01	TRUE	FALSE
ADAMTS1	11.04	-1.71	1.65E-02	-1.13	1.58E-01	TRUE	FALSE
ADAMTS2	6.53	-0.43	5.60E-01	-1.68	3.47E-02	TRUE	FALSE
ADAMTS2	6.00	-0.02	9.98E-01	-0.64	7.51E-01	FALSE	FALSE
ADAMTS3	5.56	-0.15	8.96E-01	-0.38	7.75E-01	FALSE	FALSE
ADAMTS4	4.98	-0.24	8.11E-01	-0.29	8.59E-01	FALSE	FALSE
ADAMTS4	4.89	-1.76	5.56E-01	-2.05	7.03E-01	FALSE	FALSE
ADAMTS5	8.20	-1.49	7.37E-02	-1.75	9.53E-02	FALSE	FALSE
ADAMTS6	4.92	-0.66	2.87E-01	-0.67	5.21E-01	FALSE	FALSE

ADAMTS6	4.97	0.22	9.06E-01	0.17	9.59E-01	FALSE	FALSE
ADAMTS6	4.78	0.00	1.00E+00	-0.13	9.70E-01	FALSE	FALSE
ADAMTS7	5.19	-0.25	7.24E-01	0.24	8.50E-01	FALSE	FALSE
ADAMTS7	17.19	0.36	8.78E-01	0.22	9.63E-01	FALSE	FALSE
ADAMTS7	5.27	-0.16	8.96E-01	-0.15	9.39E-01	FALSE	FALSE
ADAMTS7	9.00	0.28	8.99E-01	0.17	9.69E-01	FALSE	FALSE
ADAMTS8	4.56	0.39	4.73E-01	-0.07	9.72E-01	FALSE	FALSE
ADAMTS9	10.71	1.19	4.78E-02	0.26	8.70E-01	TRUE	FALSE
ADAMTS9-AS1	4.89	-0.24	7.40E-01	-0.45	6.81E-01	FALSE	FALSE
ADAMTS9-AS2	5.82	0.07	9.48E-01	-0.06	9.72E-01	FALSE	FALSE
ADAMTS10	5.79	0.43	6.26E-01	0.08	9.81E-01	FALSE	FALSE
ADAMTS12	4.87	0.11	9.40E-01	0.13	9.55E-01	FALSE	FALSE
ADAMTS13	8.49	1.20	1.71E-02	0.24	8.29E-01	TRUE	FALSE
ADAMTS13	5.22	0.11	9.17E-01	0.06	9.72E-01	FALSE	FALSE
ADAMTS14	5.75	1.35	1.65E-01	0.63	7.95E-01	FALSE	FALSE
ADAMTS15	4.70	-0.47	5.71E-01	-0.19	9.35E-01	FALSE	FALSE
ADAMTS16	5.07	-0.03	9.93E-01	-0.03	9.94E-01	FALSE	FALSE
ADAMTS17	7.11	-0.30	7.81E-01	-0.12	9.68E-01	FALSE	FALSE
ADAMTS17	6.78	-0.36	6.51E-01	-0.66	5.46E-01	FALSE	FALSE
ADAMTS18	5.16	-0.24	8.21E-01	-0.28	8.66E-01	FALSE	FALSE
ADAMTS19	5.52	0.07	9.67E-01	0.44	7.20E-01	FALSE	FALSE
ADAMTS20	4.72	-0.14	8.98E-01	-0.41	7.49E-01	FALSE	FALSE
ADAMTS20	4.76	-0.16	9.36E-01	-0.13	9.70E-01	FALSE	FALSE

Gene Name	A	M shCD63_49	PVal shCD63_49	M shCD63_51	PVal shCD63_51	shCD63-49	shCD63-51
ADAMTSL1	4.93	-0.22	7.62E-01	-0.27	8.22E-01	FALSE	FALSE
ADAMTSL1	5.35	-0.15	8.60E-01	-0.15	9.20E-01	FALSE	FALSE
ADAMTSL1	5.77	-0.29	6.55E-01	-0.71	3.25E-01	FALSE	FALSE
ADAMTSL1	4.88	-0.16	9.62E-01	0.89	7.50E-01	FALSE	FALSE
ADAMTSL2	5.35	-0.32	7.44E-01	0.07	9.84E-01	FALSE	FALSE
ADAMTSL2	5.36	0.22	7.82E-01	0.27	8.31E-01	FALSE	FALSE
ADAMTSL2	5.86	-0.18	8.41E-01	0.03	9.90E-01	FALSE	FALSE
ADAMTSL3	9.06	-0.67	1.68E-01	-0.32	7.87E-01	FALSE	FALSE
ADAMTSL3	6.95	-0.64	3.47E-01	-0.46	7.60E-01	FALSE	FALSE
ADAMTSL4	5.27	0.17	8.94E-01	-0.22	9.01E-01	FALSE	FALSE
ADAMTSL4	7.58	-0.44	3.85E-01	-0.50	5.48E-01	FALSE	FALSE
ADAMTSL4	7.97	-0.25	7.36E-01	-0.52	6.16E-01	FALSE	FALSE
ADAMTSL5	8.18	-0.26	7.84E-01	-0.21	9.11E-01	FALSE	FALSE
ADAMTSL5	15.03	-0.16	9.68E-01	-0.02	9.98E-01	FALSE	FALSE

Gene Name	A	M shCD63_49	PVal shCD63_49	M shCD63_51	PVal shCD63_51	shCD63-49	shCD63-51
CTSA	15.13	0.40	4.45E-01	-0.01	9.98E-01	FALSE	FALSE

CTSA	12.91	0.29	8.09E-01	-0.29	8.83E-01	FALSE	FALSE
CTSB	12.34	0.05	9.74E-01	0.04	9.89E-01	FALSE	FALSE
CTSC	10.31	0.07	9.78E-01	-0.03	9.94E-01	FALSE	FALSE
CTSC	7.71	-1.24	7.71E-02	-0.37	8.29E-01	FALSE	FALSE
CTSC	12.77	-0.50	4.10E-01	-0.53	6.19E-01	FALSE	FALSE
<b>CTSD</b>	<b>13.20</b>	<b>1.33</b>	<b>3.88E-02</b>	<b>0.70</b>	<b>5.28E-01</b>	<b>TRUE</b>	<b>FALSE</b>
CTSE	5.83	0.14	8.91E-01	0.12	9.52E-01	FALSE	FALSE
CTSF	14.25	0.54	2.80E-01	-0.39	7.20E-01	FALSE	FALSE
CTSG	5.39	-0.03	9.93E-01	0.22	9.27E-01	FALSE	FALSE
CTSH	13.69	0.44	4.11E-01	0.14	9.21E-01	FALSE	FALSE
CTSK	8.08	-0.15	9.08E-01	-0.38	7.80E-01	FALSE	FALSE
CTSL1	7.63	-0.39	5.98E-01	-0.01	9.99E-01	FALSE	FALSE
CTSL1	13.92	-0.16	8.89E-01	-0.15	9.38E-01	FALSE	FALSE
CTSL2	11.84	-0.13	9.01E-01	-0.22	8.70E-01	FALSE	FALSE
CTSL3	4.95	0.09	9.46E-01	-0.20	9.01E-01	FALSE	FALSE
CTSO	7.79	2.10	1.24E-02	0.64	6.66E-01	TRUE	FALSE
CTSS	4.85	0.06	9.86E-01	0.18	9.63E-01	FALSE	FALSE
CTSW	5.14	-0.09	9.57E-01	-0.46	7.46E-01	FALSE	FALSE
CTSZ	11.47	-0.21	7.55E-01	-0.02	9.92E-01	FALSE	FALSE
CTSZ	9.76	-0.13	9.21E-01	0.11	9.61E-01	FALSE	FALSE

Table S3 Analyses of deregulated “Upstream regulators” according to Ingenuity Pathway Analysis of microarray datasets from CD63 knock down in SKOV3ipL cells. shCD63\_49: SKOV3ipL shCD63\_49, shCD63\_51: SKOV3ipL shCD63\_51. The Z-score in each category is represented.

<b>Upstream regulators</b>	<b>shCD63_49 vs shNT</b>	<b>sh CD63_51 vs shNT</b>
beta-estradiol	-0,38	-1,66
VEGFA	-0,44	-1,79
HGF	-0,66	-1,94
<b>AKT1</b>	<b>-0,59</b>	<b>-2,18</b>
mir-21	-2,34	-2,24
ERBB4	-1,62	-0,78
<b>TGFB1</b>	<b>-1,40</b>	<b>-1,96</b>
<b>WNT3A</b>	<b>-2,03</b>	<b>-1,67</b>
MAPK1	-1,91	-1,34
<b>Tgf beta</b>	<b>-1,58</b>	<b>-1,40</b>
ERBB3	-1,57	-1,40
OSM	2,01	-1,51
HTT	1,64	-1,98
poly rl:rC-RNA	3,82	1,99
lipopolysaccharide	3,40	2,08
IRF7	3,45	2,43
TNF	2,53	2,72
MYCN	2,42	1,99
IL1B	2,40	1,82
IFNB1	2,65	1,97
EZH2	2,63	2,20
lfn	2,73	0,00

NFkB (complex)	2,84	-0,28
IKBKB	2,88	-0,45
thioacetamide	2,18	0,00
IFNA1/IFNA13	2,38	0,00
CD40LG	2,31	0,00
IFNG	3,95	1,25
IL7	2,79	
IFNA2	2,92	
Interferon alpha	3,39	
STAT1	3,23	
TLR4	3,06	
IL2	3,13	
KRAS	1,40	1,91
FGF1	1,59	1,66
STAT3	1,74	
CD40	1,75	
TNFSF12	1,78	
TNFRSF1B	1,81	
TICAM1	1,80	
ADIPOQ	1,71	
vancomycin	1,69	
IL1A	1,69	
SLC13A1	1,63	
SELPLG	1,63	
MYD88	1,65	
IL15	1,65	
plicamycin	1,67	

captopril	1,66	
EBI3	1,66	
Tnf (family)	1,59	
TNFRSF1A	1,58	
LIF	1,51	
etoposide	1,56	
Pam3-Cys-Ser-Lys4	1,53	
KLF2	1,54	
estrogen receptor	2,38	1,41
SPP1	2,61	
lomustine	2,65	
phenacetin	2,63	
IL27	2,63	
camptothecin	2,50	
IKBKG	2,31	
HNF4A	2,36	
IFNL1	2,38	
IFN alpha/beta	2,40	
CHUK	2,43	
JAK1	2,43	
DKK1	2,42	
lfn gamma	1,85	
testosterone	1,89	
SPDEF	1,91	
BCL2	1,93	
Salmonella enterica serotype abortus equi lipopolysaccharide	1,98	1,07
peptidoglycan	1,95	

NLRC5	1,95	
IL17F	1,95	
isobutylmethylxanthine	2,00	
D-galactosamine	2,00	
diclofenac	1,97	
IFNAR1	1,97	
E. coli B5 lipopolysaccharide	1,97	
OLR1	1,99	
ethionine	1,98	
TRAF6	1,98	
BAX	1,98	
3,3'-diindolylmethane	1,98	
E. coli B4 lipopolysaccharide	2,10	
IL17A	2,08	
tamoxifen	2,07	
IFN Beta	2,07	
TLR2	2,16	
RELA	2,15	
triamterene	2,14	
gentamicin C	2,14	
androgen	2,14	
allopurinol	2,14	
TLR3	2,21	
NLRP12	2,20	
E. coli lipopolysaccharide	2,19	
TNFSF10	2,19	
RET	2,19	

dimethyl sulfoxide	2,22	
FN1	2,23	
IL6	2,25	
Ni2+	2,24	
carboplatin	2,24	
STAT2	2,24	
RBPJ	2,24	
CREB1	2,24	
TRIM24	-1,71	0,00
9,10-dimethyl-1,2-benzanthracene	-1,98	0,00
prednisolone	-2,54	
SMAD4	-2,49	
alefacept	-2,45	
SMAD2	-2,43	
IL1RN	-2,12	
KIAA1524	-2,22	1,07
eicosapentenoic acid	-2,18	
SOCS1	-2,17	
tert-butyl-hydroquinone	-2,22	
TAB1	-2,22	
miR-146a-5p (and other miRNAs w/seed GAGAACU)	-2,24	
BMP6	-2,23	
methapyrilene	-1,89	
PI3K (complex)	-1,86	
SMAD3	-1,94	
nitrofurantoin	-1,91	
Mek	-1,91	

Smad	-1,96	
Insulin	-1,96	
flutamide	-1,96	
GnRH-A	-1,97	
Vegf	-1,99	
Bay 11-7082	-1,98	
thyroid hormone	-2,00	
miR-145-5p (and other miRNAs w/seed UCCAGUU)	-2,00	
MKL2	-2,00	
pyrrolidine dithiocarbamate	-1,54	
Pkc(s)	-1,53	
lysophosphatidic acid	-1,64	
CLDN7	-1,60	
TGFB2	-1,79	
IL10	-1,79	
SIRT1	-1,73	
D-glucose	-1,73	
HMOX1	-1,70	
Lh	-1,71	
CDKN2A	-1,72	
HIF1A	0,77	-1,52
LDL	0,69	-1,95
IL1	0,89	-1,97
ESR1	1,94	-0,55
CSF2	1,55	0,43
APP	1,78	0,36
valproic acid	1,67	0,13

IL4	1,55	0,15
WISP2	1,98	0,00
sulindac sulfide	1,71	0,00
IRF1	1,82	0,00

Table S4. Expression of tetraspanins based on the transcriptome analysis from SKOV3ipL cell lines. SKOV3ipL shCD63\_51. Logarithm (base 2) of the average intensity and logarithm (base 2) of the ratio (shCD63 vs shNT) as well as corresponding adjusted p-values are represented. A: Mean expression of intensity. M: Mean ratio shCD63 vs. shNT. P-Val: p-values. TRUE/FALSE: Last two columns represent if the modulation of certain gene is significant („True“) concerning cut off values of A>6, absolute value of M> 0,7 and pVal< 0,05. „False“ represents no significant modulation according to adjusted cut-off values. shCD63\_49: SKOV3ipL shCD63\_49, shCD63\_51: SKOV3ipL shCD63\_51.

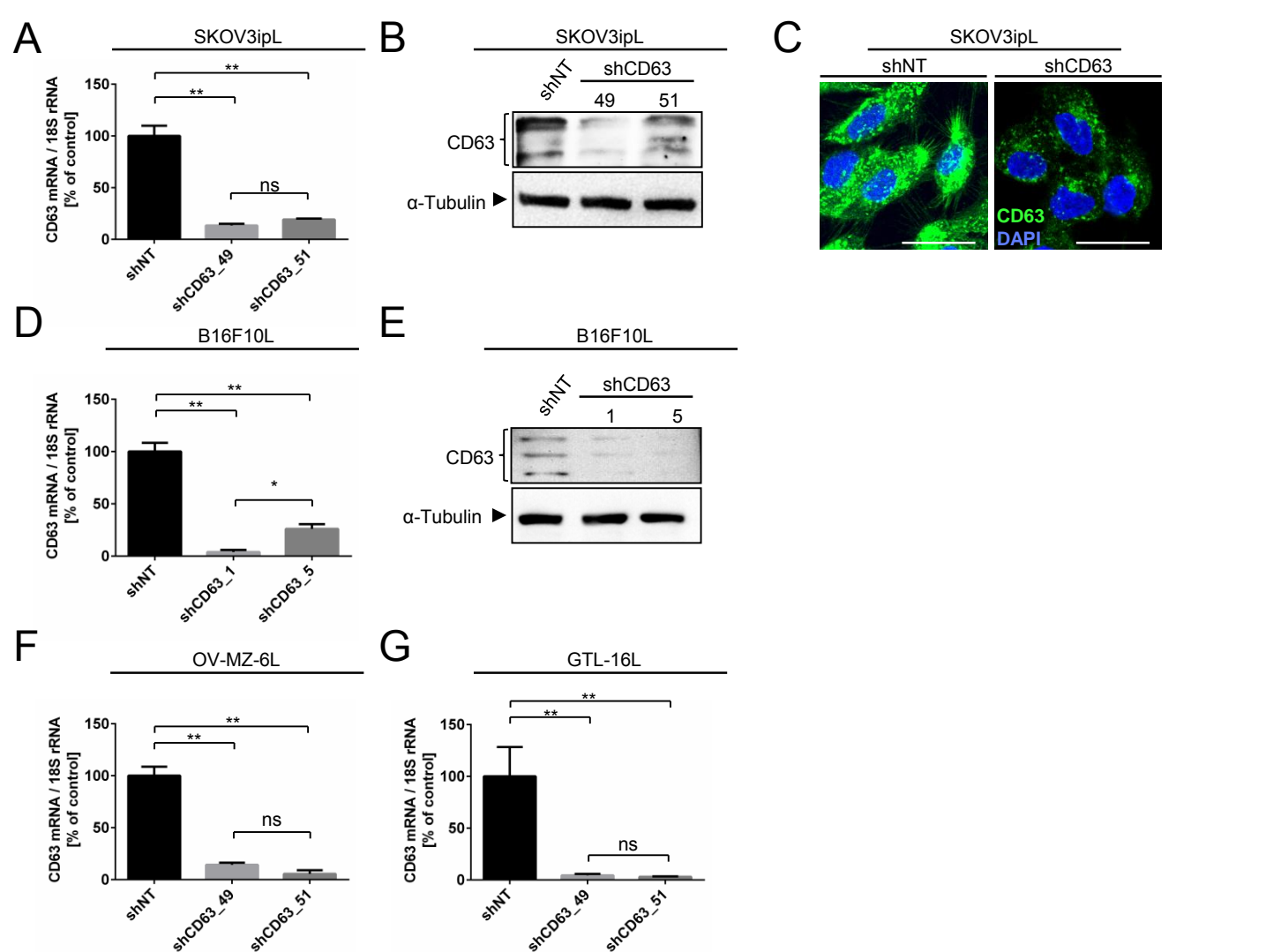
Gene Name	A	M shCD63_49	PVal shCD63_49	M shCD63_51	PVal shCD63_51	shCD63-49	shCD63-51
<b>TSPAN1</b>	<b>15.26</b>	<b>1.64</b>	<b>2.68E-02</b>	<b>1.21</b>	<b>1.83E-01</b>	<b>TRUE</b>	<b>FALSE</b>
TSPAN2	5.41	-0.03	9.90E-01	-0.10	9.72E-01	FALSE	FALSE
TSPAN3	13.70	0.18	8.66E-01	0.21	8.99E-01	FALSE	FALSE
TSPAN4	15.24	0.42	4.46E-01	0.17	9.09E-01	FALSE	FALSE
TSPAN4	14.26	0.38	4.46E-01	0.11	9.40E-01	FALSE	FALSE
<b>TSPAN5</b>	<b>11.01</b>	<b>-1.31</b>	<b>4.43E-02</b>	<b>-0.41</b>	<b>7.92E-01</b>	<b>TRUE</b>	<b>FALSE</b>
TSPAN6	12.26	0.36	6.06E-01	0.12	9.56E-01	FALSE	FALSE
TSPAN7	5.02	0.59	2.91E-01	-0.05	9.84E-01	FALSE	FALSE
TSPAN8	5.05	0.08	9.58E-01	0.35	8.02E-01	FALSE	FALSE
TSPAN9	8.30	0.10	9.64E-01	-0.20	9.39E-01	FALSE	FALSE
TSPAN9	4.75	0.06	9.76E-01	0.10	9.71E-01	FALSE	FALSE
TSPAN10	7.31	0.05	9.84E-01	0.22	9.19E-01	FALSE	FALSE
TSPAN10	8.13	-0.02	9.94E-01	-0.09	9.73E-01	FALSE	FALSE
TSPAN11	5.23	-0.89	5.15E-01	-0.97	7.00E-01	FALSE	FALSE
TSPAN11	8.29	0.08	9.72E-01	0.01	9.98E-01	FALSE	FALSE
TSPAN12	8.14	-0.28	7.93E-01	0.13	9.61E-01	FALSE	FALSE
TSPAN13	8.66	-0.22	8.15E-01	-1.14	1.15E-01	FALSE	FALSE
TSPAN14	9.36	-0.30	7.20E-01	-0.86	3.09E-01	FALSE	FALSE
TSPAN14	11.61	-0.11	9.41E-01	-0.52	6.74E-01	FALSE	FALSE
TSPAN14	12.97	0.40	7.08E-01	0.15	9.61E-01	FALSE	FALSE
TSPAN14	8.29	-0.11	9.65E-01	-0.34	8.74E-01	FALSE	FALSE
TSPAN15	10.53	0.41	6.38E-01	0.49	7.54E-01	FALSE	FALSE
TSPAN16	5.04	0.12	9.19E-01	0.09	9.66E-01	FALSE	FALSE
TSPAN17	8.46	0.08	9.72E-01	-0.48	7.98E-01	FALSE	FALSE
TSPAN17	10.23	0.11	9.34E-01	-0.31	8.09E-01	FALSE	FALSE
TSPAN18	8.72	-0.24	8.92E-01	-0.20	9.52E-01	FALSE	FALSE
TSPAN19	5.45	1.15	5.87E-01	-0.26	9.71E-01	FALSE	FALSE

Table S5. Expression of integrins based on the transcriptome analysis from SKOV3ipL cell lines. Logarithm (base 2) of the average intensity and logarithm (base 2) of the ratio (shCD63 vs shNT) as well as corresponding adjusted p-values are represented. A: Mean expression of intensity. M: Mean ratio shCD63 vs. shNT. P-Val: p-values. TRUE/FALSE: Last two columns represent if the modulation of certain gene is significant („True“) concerning cut off values of A>6, absolute value of M> 0,7 and pVal< 0,05. „False“ represents no significant modulation according to adjusted cut-off values. shCD63\_49: SKOV3ipL shCD63\_49, shCD63\_51: SKOV3ipL shCD63\_51.

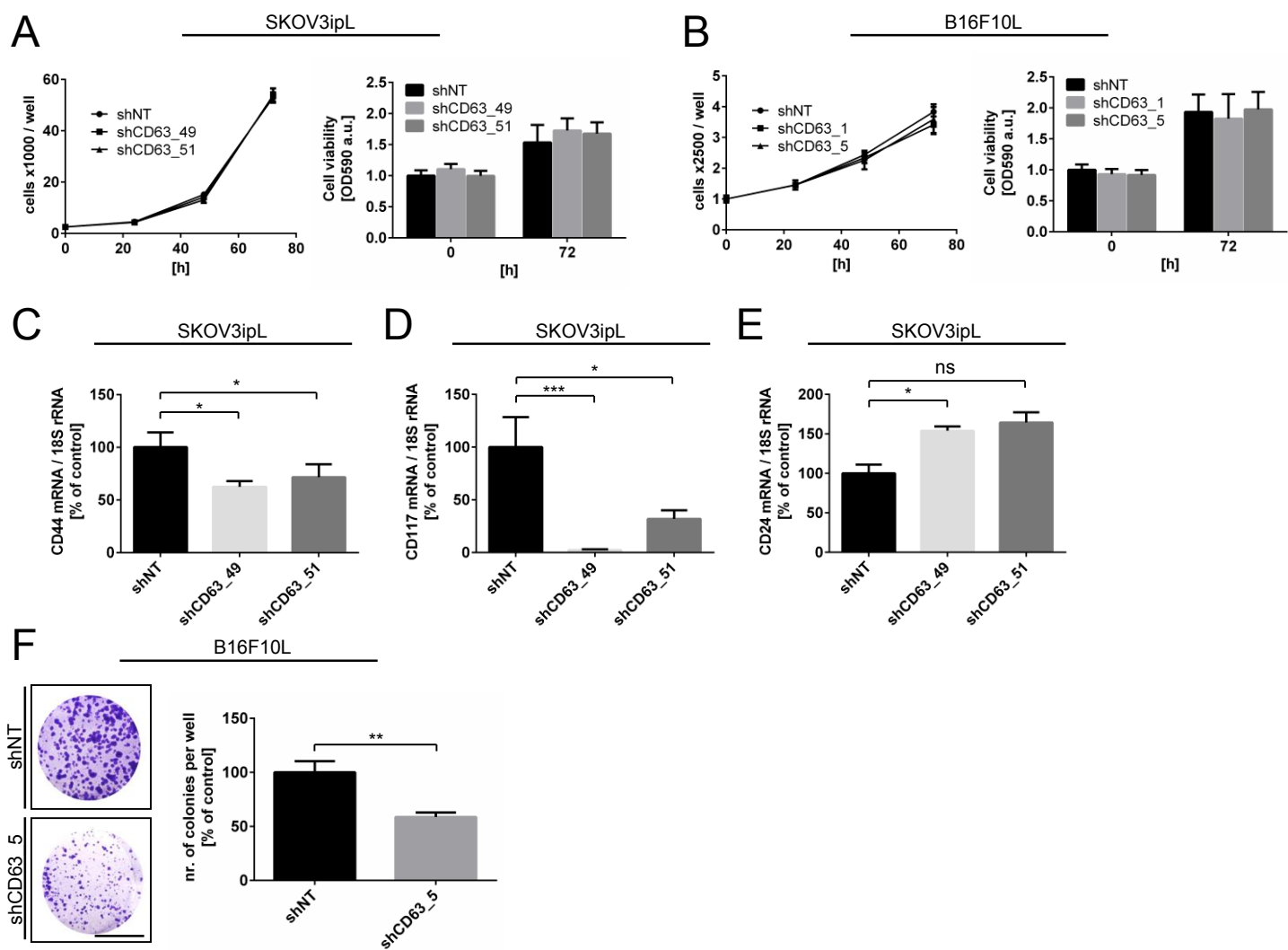
Gene Name	A	M shCD63_49	PVal shCD63_49	M shCD63_51	PVal shCD63_51	shCD63-49	shCD63-51
ITGA1	7.57	-0.16	8.94E-01	0.71	4.40E-01	FALSE	FALSE
ITGA2	4.91	-0.42	4.42E-01	0.03	9.89E-01	FALSE	FALSE
ITGA3	14.12	-0.06	9.82E-01	0.51	7.73E-01	FALSE	FALSE
ITGA4	5.81	-0.21	8.22E-01	0.20	9.06E-01	FALSE	FALSE
ITGA4	6.12	-0.35	7.82E-01	0.84	5.91E-01	FALSE	FALSE
ITGA4	7.34	-0.38	7.02E-01	1.01	3.37E-01	FALSE	FALSE
ITGA5	9.82	0.46	5.35E-01	0.73	4.76E-01	FALSE	FALSE
ITGA6	8.64	-0.54	3.87E-01	0.43	7.41E-01	FALSE	FALSE
ITGA6	10.37	-0.65	3.41E-01	0.56	6.87E-01	FALSE	FALSE
ITGA7	10.50	0.57	2.59E-01	-0.46	6.46E-01	FALSE	FALSE
ITGA8	4.96	-0.81	6.70E-01	-0.39	9.35E-01	FALSE	FALSE
ITGA9	6.93	-0.27	8.89E-01	0.15	9.71E-01	FALSE	FALSE
ITGA10	8.02	0.02	9.94E-01	0.17	9.12E-01	FALSE	FALSE
ITGA11	6.11	-0.28	7.48E-01	-0.12	9.61E-01	FALSE	FALSE
ITGAD	4.78	0.08	9.74E-01	0.09	9.81E-01	FALSE	FALSE
ITGAD	5.34	0.48	7.14E-01	-0.01	9.99E-01	FALSE	FALSE
ITGAE	11.63	-0.32	7.17E-01	-0.15	9.46E-01	FALSE	FALSE
ITGAL	4.77	0.07	9.62E-01	-0.17	9.20E-01	FALSE	FALSE
ITGAM	5.55	-0.13	9.27E-01	0.16	9.35E-01	FALSE	FALSE
<b>ITGAV</b>	<b>11.82</b>	<b>0.04</b>	<b>9.89E-01</b>	<b>0.59</b>	<b>6.41E-01</b>	<b>FALSE</b>	<b>FALSE</b>
ITGAX	5.07	0.71	2.01E-01	-0.16	9.32E-01	FALSE	FALSE
<b>ITGB1</b>	<b>11.92</b>	<b>-0.24</b>	<b>8.65E-01</b>	<b>0.21</b>	<b>9.30E-01</b>	<b>FALSE</b>	<b>FALSE</b>
ITGB2	8.68	0.51	4.29E-01	-0.36	7.99E-01	FALSE	FALSE
<b>ITGB3</b>	<b>9.98</b>	<b>0.77</b>	<b>1.88E-01</b>	<b>-0.07</b>	<b>9.78E-01</b>	<b>FALSE</b>	<b>FALSE</b>
ITGB4	11.86	0.56	3.98E-01	0.86	3.10E-01	FALSE	FALSE
ITGB5	13.94	-0.41	5.35E-01	-0.15	9.34E-01	FALSE	FALSE
ITGB6	5.92	-0.43	8.04E-01	-0.18	9.68E-01	FALSE	FALSE
ITGB7	9.62	0.46	3.98E-01	0.52	5.72E-01	FALSE	FALSE
ITGB8	8.55	0.81	1.42E-01	0.27	8.46E-01	FALSE	FALSE

Table S6. Summary of genes belonging to proteases and tetraspanin families which are regulated by CD63 knock down according to microarray analysis. shCD63\_49: SKOV3ipL shCD63\_49, shCD63\_51: SKOV3ipL shCD63\_51. Logarithm (base 2) of the average intensity and logarithm (base 2) of the ratio (shCD63 vs shNT) as well as corresponding adjusted p-values are represented.

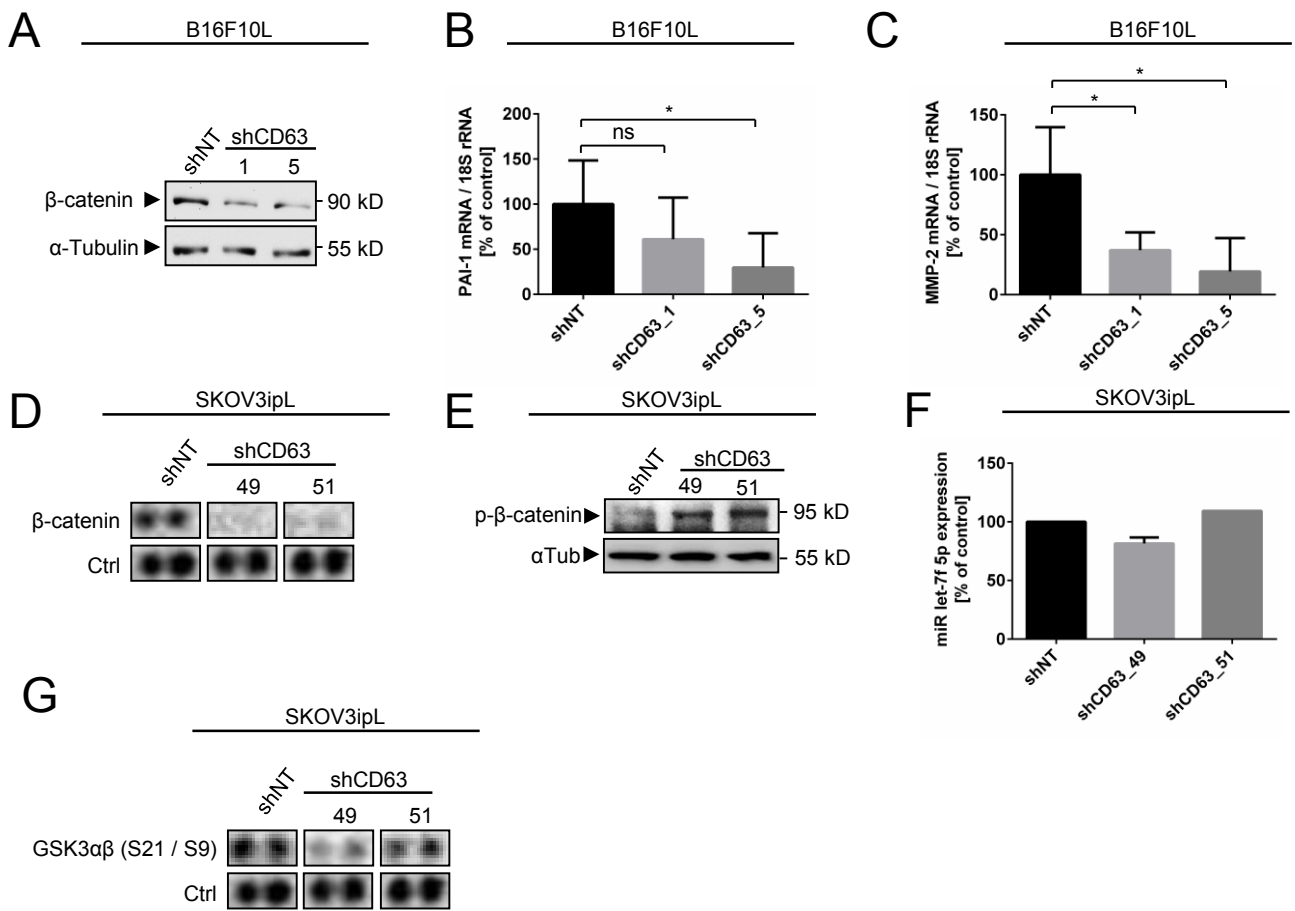
Gene Name	Log2 Average	Log Ratio shCD63_49	p-value shCD63_49	Log Ratio shCD63_51	p-value shCD63_51
ADAM23	6.723	-0.543	2.70E-01	-1.622	1.88E-02
<b>ADAMTS1</b>	<b>9.701</b>	<b>-1.832</b>	<b>1.31E-02</b>	<b>-1.183</b>	<b>1.41E-01</b>
ADAMTS2	6.531	-0.434	5.60E-01	-1.682	3.47E-02
ADAMTS9	10.714	1.194	4.78E-02	0.261	8.70E-01
ADAMTS13	8.487	1.199	1.71E-02	0.236	8.29E-01
C3	11.083	3.899	1.99E-03	1.578	5.09E-02
CFB	10.086	1.791	1.31E-02	0.956	2.53E-01
CFD	13.928	0.504	3.92E-01	-0.128	9.48E-01
<b>CTSD</b>	<b>13.2</b>	<b>1.326</b>	<b>3.88E-02</b>	<b>0.7</b>	<b>5.28E-01</b>
CTSG	5.394	-0.029	9.93E-01	0.215	9.27E-01
CTSO	7.786	2.103	1.24E-02	0.638	6.66E-01
DPP4	11.425	1.342	3.80E-02	1.114	1.70E-01
ICAM2	8.128	2.202	1.78E-02	2.534	2.41E-02
MMP1	11.643	1.193	4.28E-02	0.803	3.38E-01
<b>MMP7</b>	<b>7.776</b>	<b>2.183</b>	<b>3.02E-02</b>	<b>0.831</b>	<b>6.92E-01</b>
NPEPPS	11.097	1.12	4.52E-02	1.012	1.50E-01
PLAU	15.189	0.672	3.12E-01	1.162	1.47E-01
PREPL	9.609	-1.11	2.45E-02	0.363	8.91E-01
SERPINE1	9.686	-1.72	4.13E-02	-2.37	3.18E-02
SLPI	13.4	2.412	4.51E-03	1.741	3.20E-02
TFPI	9.458	1.658	2.42E-02	0.304	8.67E-01
<b>TSPAN1</b>	<b>15.257</b>	<b>1.639</b>	<b>2.68E-02</b>	<b>1.21</b>	<b>1.83E-01</b>
<b>TSPAN5</b>	<b>11.013</b>	<b>-1.314</b>	<b>4.43E-02</b>	<b>-0.413</b>	<b>7.92E-01</b>
TSPAN33	10.401	1.191	3.39E-02	-0.632	4.89E-01



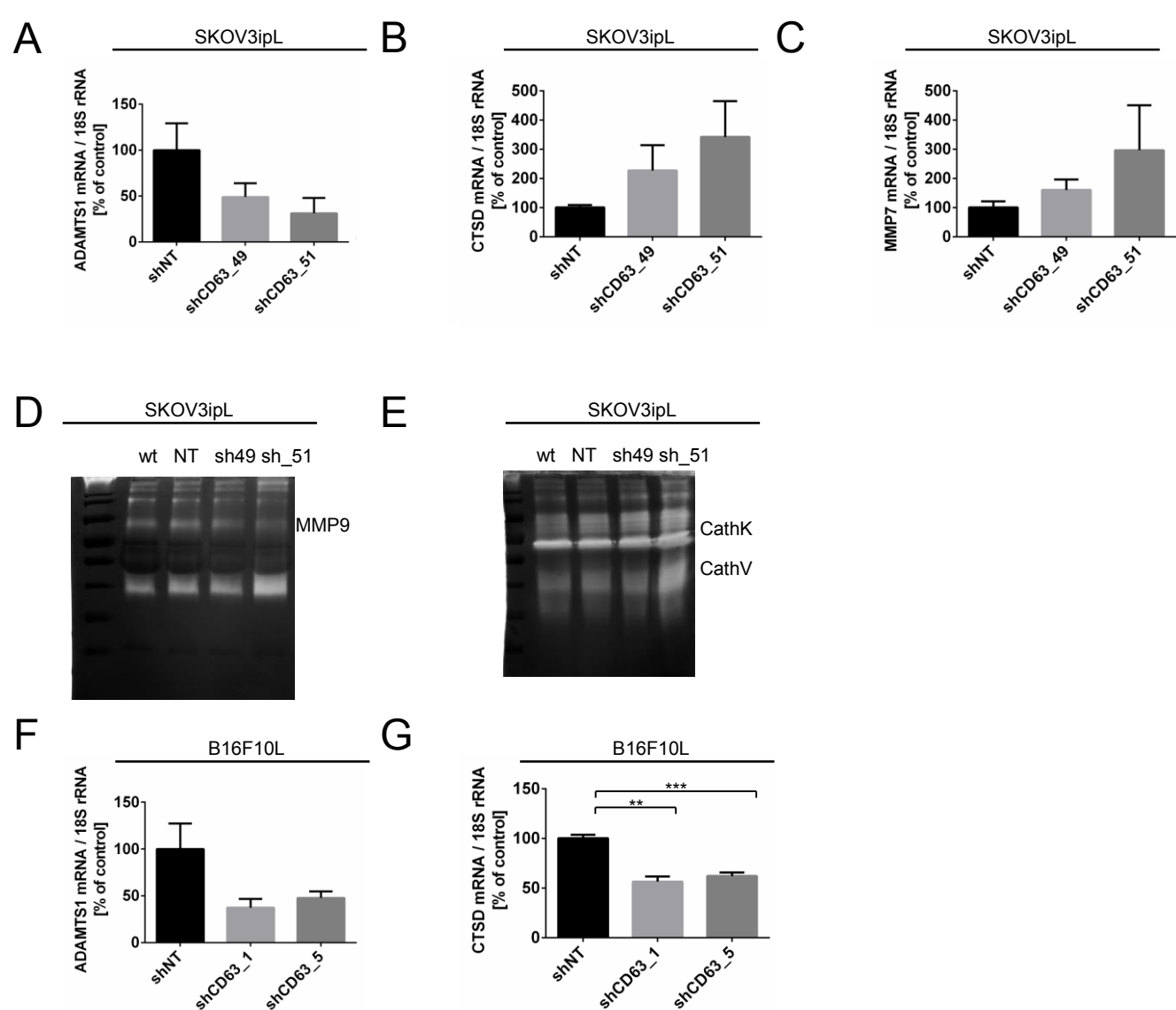
**Supplementary Figure 1: Knock down of CD63 in different tumor cell lines.** (A-C) CD63 levels in the human ovarian carcinoma cell line SKOV3ip were assessed after infection with lentiviral vectors coding for CD63-specific shRNA (shCD63\_49, shCD63\_51) or non-target control (shNT.), respectively. CD63 was assessed on mRNA level using qRT-PCR (A) and on protein level using Western blot (B) and immunocytochemistry (C). (B)  $\alpha$ -Tubulin was used as a loading control. (C) Representative pictures are shown. DAPI was used as a counterstaining. Bars, 25  $\mu$ m. (D, E) CD63 levels in the murine melanoma cell line are decreased upon infection with lentiviral vectors coding for CD63-specific shRNA (shCD63\_1, shCD63\_5) or non-target control (shNT.), respectively. CD63 was assessed on mRNA level using qRT-PCR (D) and on protein level using Western blot (E). (E)  $\alpha$ -Tubulin was used as a loading control. (F) CD63 levels in the human ovarian carcinoma cell line OV-MZ-6L are decreased upon infection with lentiviral vectors coding for CD63-specific shRNA (shCD63\_49, shCD63\_51) or non-target control (shNT.), respectively. CD63 was assessed on mRNA level using qRT-PCR. (G) CD63 levels in the human gastric cancer cell line GTL-16L are decreased upon infection with lentiviral vectors coding for CD63-specific shRNA (shCD63\_49, shCD63\_51) or non-target control (shNT.), respectively. CD63 was assessed on mRNA level using qRT-PCR. (A, D, F, G) Target mRNA is shown relative to 18S rRNA and normalized to the respective control (shNT). Results are mean + SEM (error bars)  $n = 3$ . \*\* $P \leq 0001$ , unpaired  $t$  test.



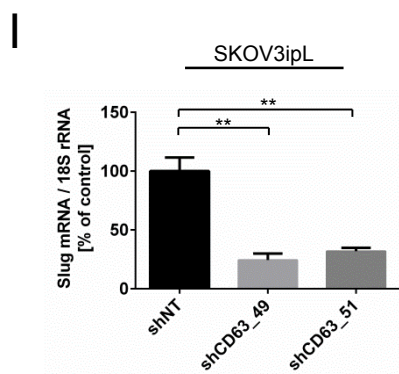
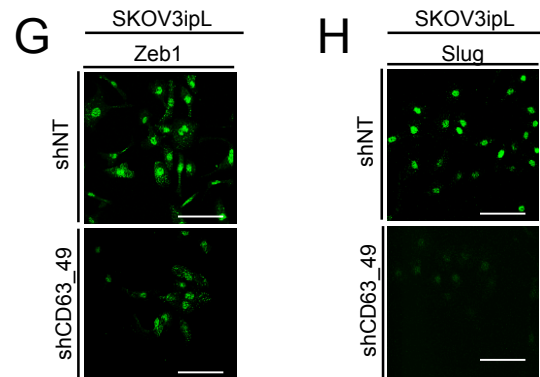
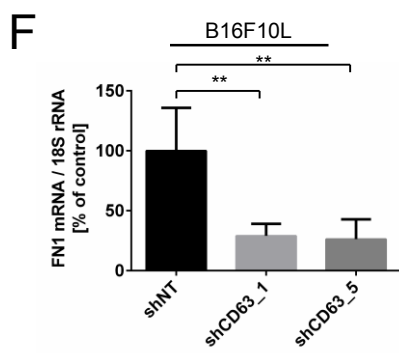
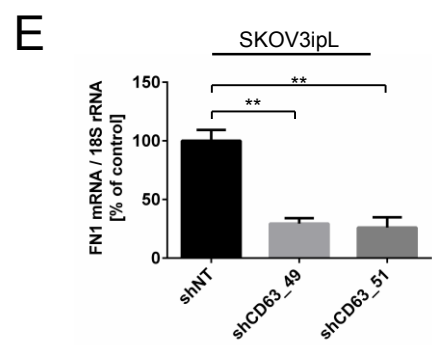
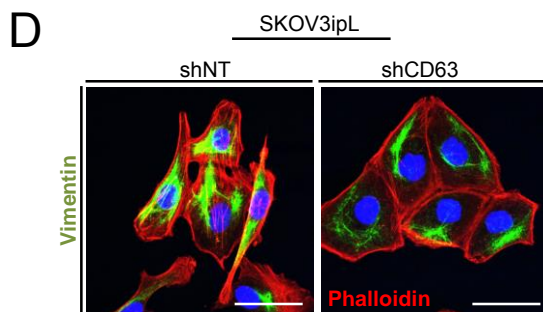
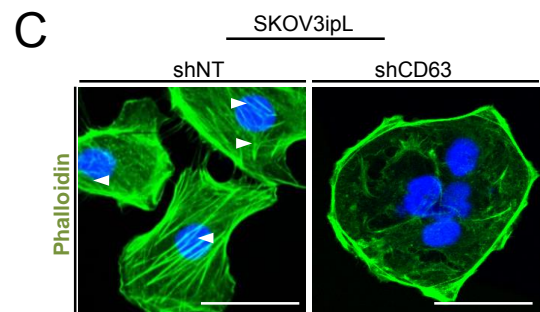
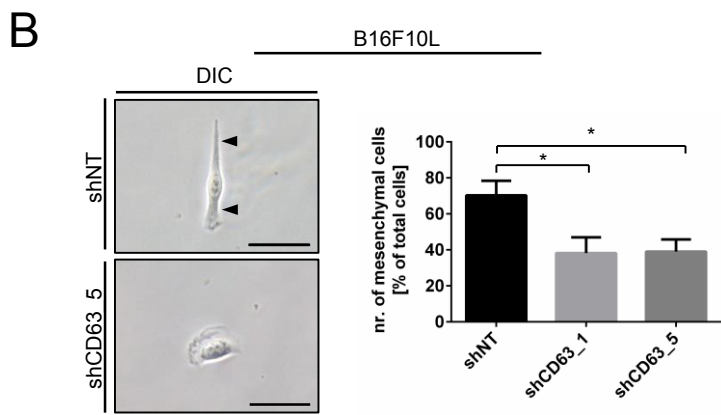
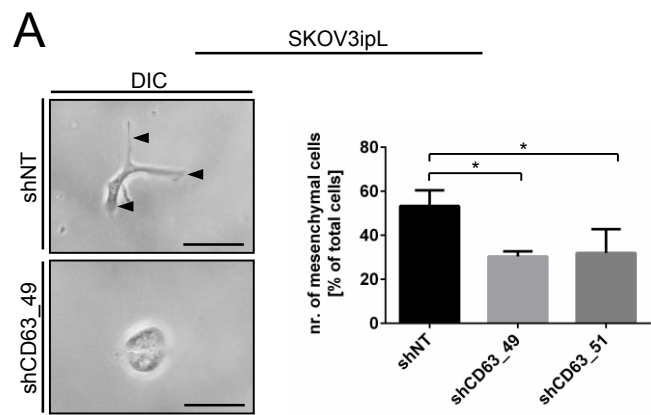
**Supplementary Figure 2. Cell proliferation is unaltered upon CD63 knock down while stem cell markers are decreased.** (A, B) CD63 knock down does not alter cell proliferation. Cell viability was assessed using an Alamar blue assay. (C-E) Stem cell marker CD44 and CD117 are reduced on mRNA level while CD24 is increased upon CD63 knock down. Target mRNA is shown relative to 18S rRNA and normalized to the respective control (shNT). (F) Clonogenic assay using B16F10L cells show decreased colony formation upon CD63 knock down. Representative pictures (left panel). Bar, 1 cm.. (A-F): Results are shown as mean + SEM (error bars). \* $P \leq 0.05$ ; \*\* $P \leq 0.01$ ; \*\*\* $P \leq 0.001$ ; unpaired t test. (n = 3). (A-F): shNT: cell lines stably transduced with non-target shRNA control. shCD63: cell lines stably transduced with shRNA against CD63.



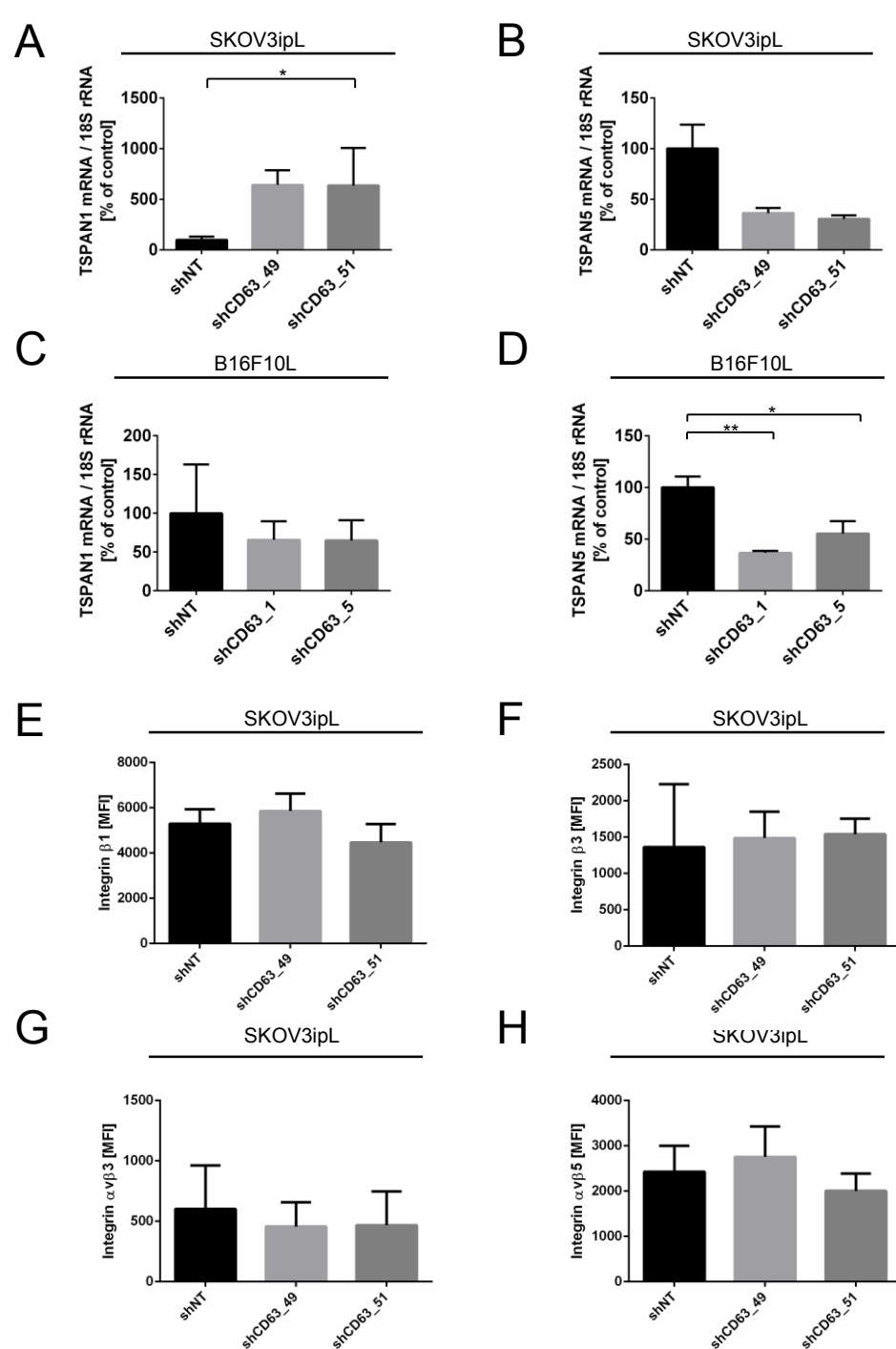
**Supplementary Figure 3. β-catenin and β-catenin target proteins are reduced upon CD63 knock down.** (A) β-catenin levels are reduced on protein level upon CD63 knock down in B16F10L murine melanoma cells. Quantification of β-catenin on protein level was done using Western blot. α-Tubulin was used as a loading control. (B, C) β-catenin targets Pai-1 and Mmp-2 are reduced upon CD63 knock down in B16F10L cells. Quantification of the direct β-catenin transcriptional target Pai-1 (A) or Mmp-2 (B) on mRNA levels was done using qRT-PCR. Target mRNA is shown relative to 18S rRNA and normalized to the respective control (shNT). (D) β-catenin levels are reduced on protein level upon CD63 knock down in SKOV3ipL cells. Quantification of β-catenin on protein level was done using a Phosphokinasearray. (E) Levels of phosphorylated β-catenin are increased on protein level upon CD63 knock down in SKOV3ipL cells. Quantification of β-catenin on protein level was done using Western blot. α-Tubulin was used as a loading control. (F) let7f 5p microRNA levels are not influenced by CD63 knock down. let7f5p-levels were assessed using a microRNA array. (G) Levels of phosphorylated GSK3αβ (S21 / S9) are reduced on protein level upon CD63 knock down in SKOV3ipL cells. Quantification of GSK3αβ on protein level was done using a Phosphokinasearray. (A-C): Results are shown as mean + SEM (error bars). \* $P \leq 0.05$ ; unpaired t test. (n = 3). (A-F) shNT: cell lines stably transduced with non-target shRNA control. shCD63: cell lines stably transduced with shRNA against CD63.



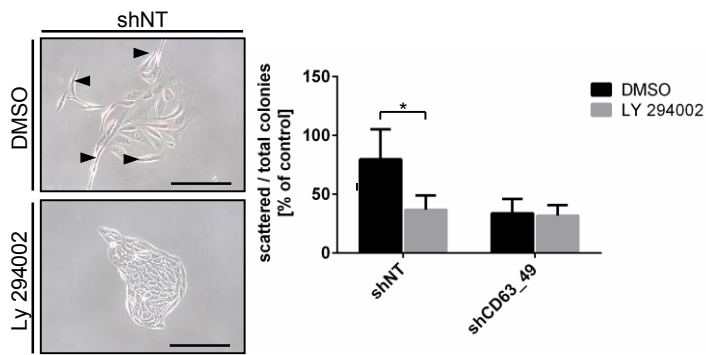
**Supplementary Figure 4: Effect of CD63 knock down on proteases.** (A-C) ADAMTS1 (A), CTSD (B, Cathepsin D) and MMP7 (C) levels in the human ovarian carcinoma cell line SKOV3ip following knock down of the tetraspanin CD63. ADAMTS1, CTSD and MMP7 mRNA levels were assessed using qRT-PCR. (D, E) MMP (D) and Cathepsin (E) zymography were done using gelatine-containing gels to assess protease activity. (F, G) ADAMTS1, CTSD (Cathepsin D) and MMP7 levels in the murine melanoma cell line B16F10L following knock down of the tetraspanin CD63. ADAMTS1 and CTSD mRNA levels were assessed using qRT-PCR. MMP7 could not be detected. TSPAN1 and TSPAN5 levels in the murine melanoma cell line following knock down of the tetraspanin CD63. (A-C, F, G) mRNA levels were assessed using qRT-PCR. Target mRNA is shown relative to 18S rRNA and normalized to the respective control (*shNT*). Results are mean + SEM (*error bars*)  $n = 3$



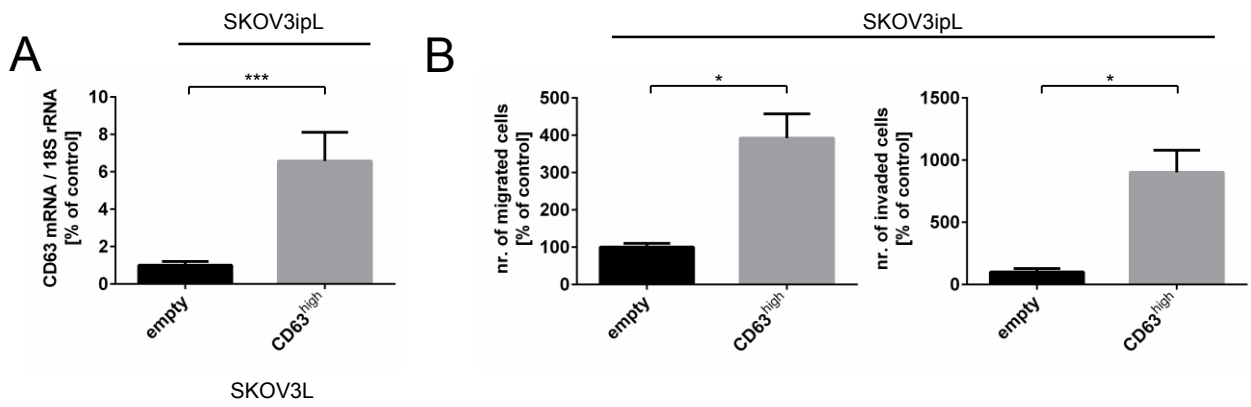
**Supplementary Figure 5. Cell morphology and EMT marker change upon CD63 knock down.** (A, B) Cell shape changes to a more epithelial phenotype upon CD63 knock down in human ovarian carcinoma SKOV3ipL (A) and murine melanoma B16F10L cells. Representative DIC pictures are shown on the left side, quantification was done based on cell shape. (C) Cytoskeleton changes upon CD63 knock down are visualized by Phalloidin-based staining of Actin. Stress fibers are reduced upon CD63 knock down. DAPI was used as a counterstaining. *Bar*, 25  $\mu$ M. (D) Vimentin expression is reduced upon CD63 knock down. Vimentin was visualized using immunocytochemistry, DAPI and Phalloiding were used as counterstaining. *Bar*, 25  $\mu$ m. (E, F) Quantification of Fibronectin on mRNA levels was done using qRT-PCR in SKOV3ipL (E) and B16F10L (F) cells. (G, H) E-Cadherin suppressors Zeb1 (G) and Snail (H) are reduced upon CD63 knock down. Zeb1 and Slug were visualized using immunocytochemistry. *Bar*, 100  $\mu$ m. (I) Quantification of E-cadherin suppressor Slug on mRNA levels was done using qRT-PCR. (E, F, I) Target mRNA is shown relative to 18S rRNA and normalized to the respective control (shNT). (A, B, E, F, I): Results are shown as mean + SEM (error bars). \* $P \leq 0.05$ ; unpaired t test. ; \*\* $P \leq 0.01$  (n = 3). (A-I) *shNT*: cell lines stably transduced with non-target shRNA control. *shCD63*: cell lines stably transduced with shRNA against CD63.



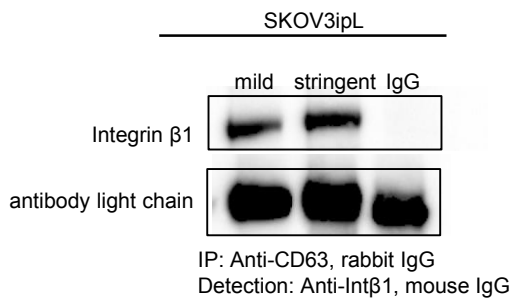
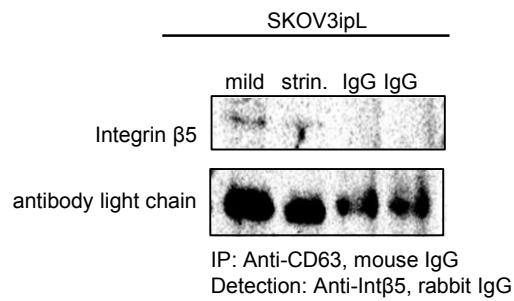
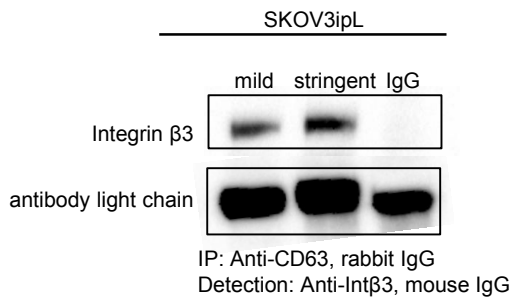
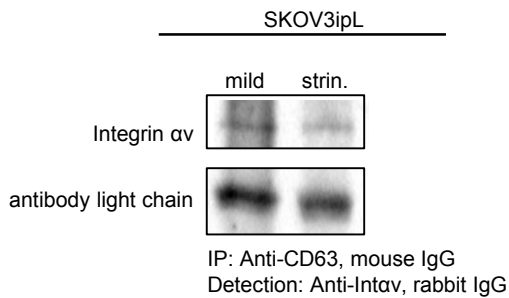
**Supplementary Figure 6: Effect of CD63 knock down on other tetraspanins and integrins and integrin dimers..** (A, B) TSPAN1 and TSPAN5 levels in the human ovarian carcinoma cell line SKOV3ip following knock down of the tetraspanin CD63. TSPAN1 and TSPAN5 mRNA levels were assessed using qRT-PCR. (C, D) TSPAN1 and TSPAN5 levels in the murine melanoma cell line B16F10L following knock down of the tetraspanin CD63. (A-D) TSPAN1 and TSPAN5 mRNA levels were assessed using qRT-PCR. Target mRNA is shown relative to 18S rRNA and normalized to the respective control (*shNT*). Results are mean + SEM (*error bars*)  $n = 3$  (E-H) Integrin  $\beta$ 1 (A), Integrin  $\beta$ 3 (B), Integrin  $\beta$ 5 (C) and Integrin  $\alpha$ v (D) protein levels verified by FACS. Data are shown as mean fluorescence intensity (MFI). Results are mean + SEM (*error bars*)  $n = 3$



**Supplementary Figure 7. Inhibition of PI3K/AKT signaling mimics CD63 knock down.** Inhibition of PI3K mimics CD63 knock down. SKOV3ip cells were incubated with Ly294002 and cell colony shape was evaluated. Results are shown as mean + SEM (error bars). \* $P \leq 0.05$ ; unpaired t test. (n = 5). *shNT*: cell lines stably transduced with non-target shRNA control. *shCD63*: cell lines stably transduced with shRNA against CD63.



**Supplementary Figure 8. Cell migration and invasion are increased upon CD63 overexpression and metastasis formation is enhanced.** (A) Verification of CD63 overexpression. CD63 levels in the human ovarian carcinoma cell line SKOV3ip were assessed after infection with lentiviral vectors coding for CD63 (CD63<sup>high</sup>), an empty vector control (empty), respectively. CD63 was assessed on mRNA level using qRT-PCR Target mRNA is shown relative to 18S rRNA and normalized to the respective control (*empty*). (B) Cell migration and *in vitro* invasion were assessed using transwell migration assays. Invasive properties were evaluated using Matrigel-coated transwells. Cell migration and *in vitro* invasion were increased upon CD63 overexpression in human ovarian carcinoma SKOV3ipL.

**A****B****C****D**

**Supplementary Figure 9: Interaction of CD63 with different integrins.** (A-D) Interaction of CD63 with different integrins was shown using immunoprecipitation. Two different CD63 antibodies were used to avoid using antibodies from the same species for capture and detection. Brij98 was used for mild conditions, NP-40 was used for more stringent conditions (strin.). IgG: isotype control. Cross reactivity with the antibody light chain was used as a loading control.